Electronic Supplementary Material (ESI) for Faraday Discussions.

ELECTRONIC SUPPLEMENTARY INFORMATION

New bio-based monomers: Tuneable polyester properties using branched diols from biomass

Sacha Pérocheau Arnaud,[a] Linglin Wu,[b] Maria-Angelica Wong Chang,[b] James W. Comerford,[a] Thomas J. Farmer,[a,]* Maximilian Schmid,[a] Fei Chang,[b] Zheng Li[b] and Mark Mascal [b,]*

[a] *Green Chemistry Centre of Excellence, Department of Chemistry, University of York, YO10 5DD, UK, *Email: thomas.farmer@york.ac.uk*
[b] *Department of Chemistry, University of California Davis, 1 Shields Avenue, Davis, CA 95616, USA, *Email: mjmascal@ucdavis.edu*

Table of Contents

The original raw data associated with this research, including GPC data and reports, is available on request at:

DOI: 10.15124/20fccc77-5902-42cc-adb9-8e58cf27bac0

Effect of MeOH washes on TGA of polyesters

Figure S1. Effect of an extra MeOH wash on P-**3**-**15** polyester from the reaction of FDCC (**3**) and isosorbide (**15**). Evidence of impurity (assumed PyCl salt) at 140-200 °C.

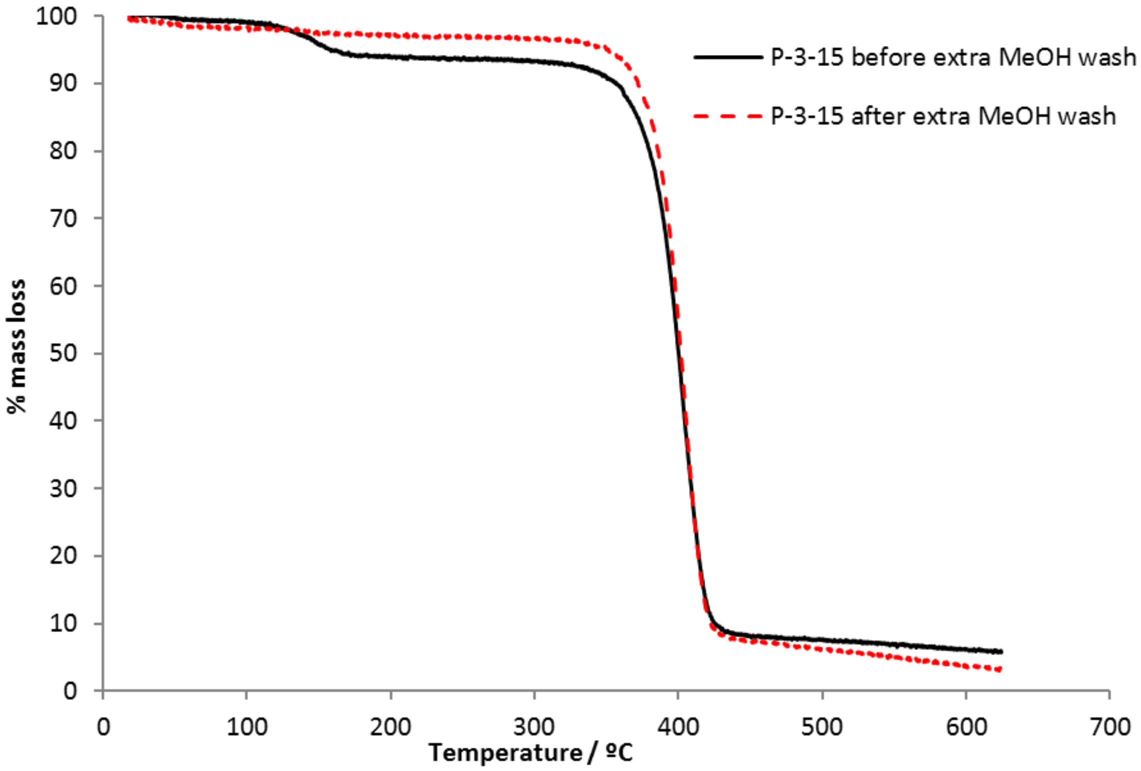

Table of literature T_gs for relevant aliphatic and aromatic polyesters

Table S1. Comparison of the glass transition temperature (T_g) of 2,7-octanediol polyesters and other previously reported aliphatic-aromatic polyesters and aliphatic-aliphatic polyesters

Diacid unit	**Diol unit**	**T_g / °C**	**Source**
Terephthalic acid (TA)	1,4-butanediol	41	[S1]
	2,3-butanediol	127, **101**	[S2], **this work**
	1,6-hexanediol	6	[S3]
	2,5-hexanediol	**65**	**This work**
	1,8-octanediol	5	[S3]
	2,7-octanediol	**63**	**This work**
	isosorbide	155, 197, **170**	[S4, S5], **this work**
2,5-furandicarboxylic acid (FDCA)	1,4-butanediol	26-36	[S6]
	2,3-butanediol	87, **84**	[S7], **this work**
	1,6-hexanediol	12-16	[S6]
	2,5-hexanediol	**56**	**This work**
	1,8-octanediol	6-13	[S6]
	2,7-octanediol	**40**	**This work**
	isosorbide	173, **153**	[S8], **this work**
Adipic acid	1,4-butanediol	n.d. (crystalline)	[S9]
	2,3-butanediol	-23, **-43**	[S9], **this work**
Sebacic acid	1,6-hexanediol	-62	[S10]
	2,5-hexanediol	-69	[S10]

Example calculation of %iso for CP-3-15-7

Figure S2. Example of calculation of %iso using the ^{1}H-NMR spectra ($CDCl_3$) of CP-**3-15-7**

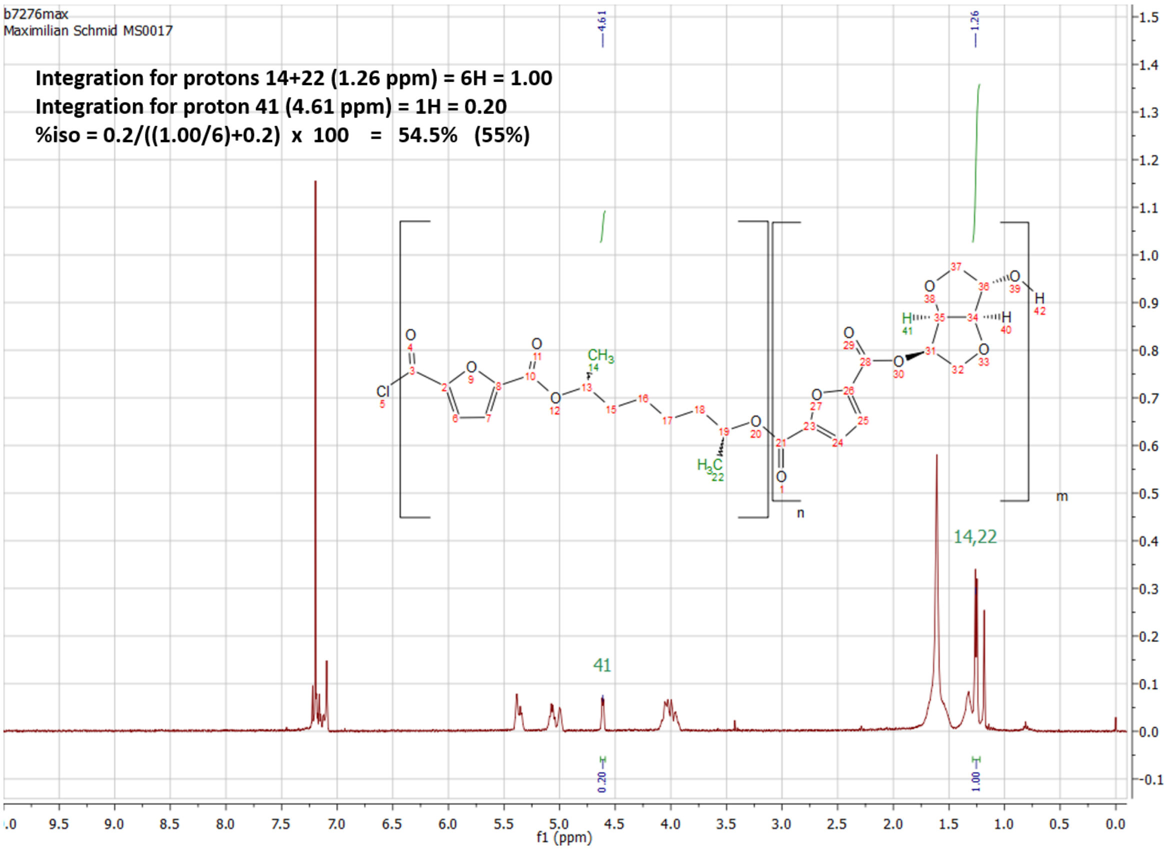

Integration for protons 14+22 (1.26 ppm) = 6H = 1.00
Integration for proton 41 (4.61 ppm) = 1H = 0.20
%iso = 0.2/((1.00/6)+0.2) x 100 = 54.5% (55%)

Comparison of TGA traces of co-polymers of 13 with 15 and diols (7, 10 and 14)

Figure S3. Comparison of TGA traces for co-polymers of isosorbide (**15**) and secondary diols (**14**, **10** or **7**) with **13**

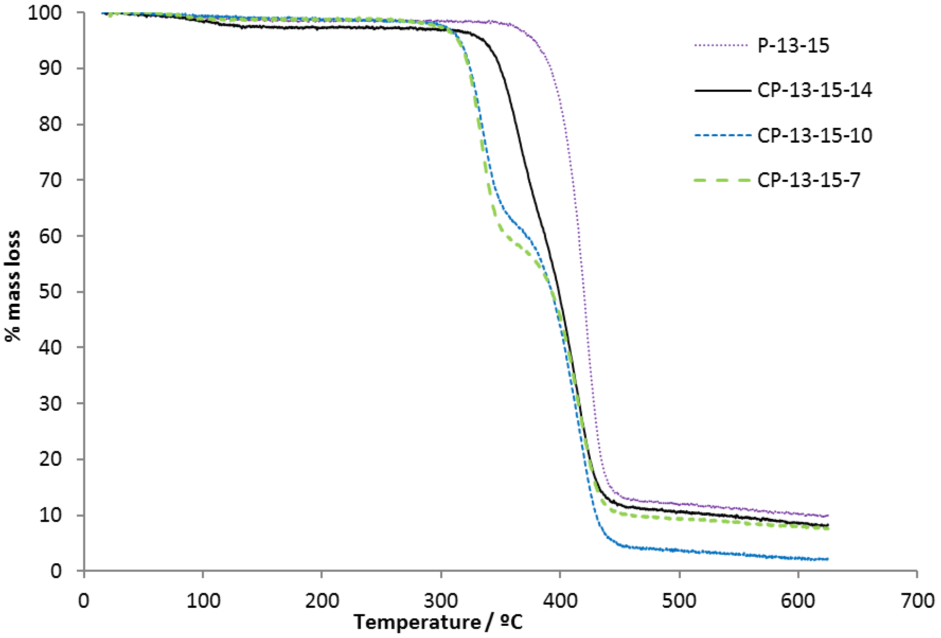

^{1}H NMR spectra of polymers

Figure S4a. ^{1}H NMR spectrum of P-**13-14**

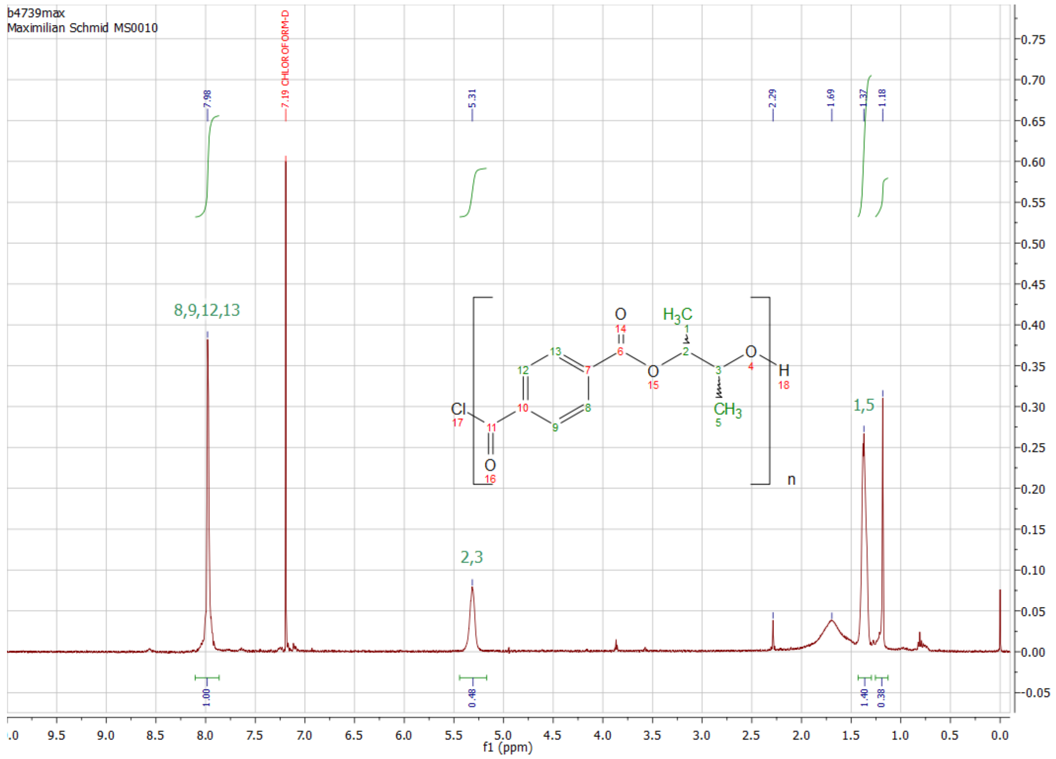

$CDCl_3$ solvent, 400 MHz, TMS reference, peak at ~1.7 ppm includes HOD

Figure S4b. ^{1}H NMR spectrum of P-**13-10**

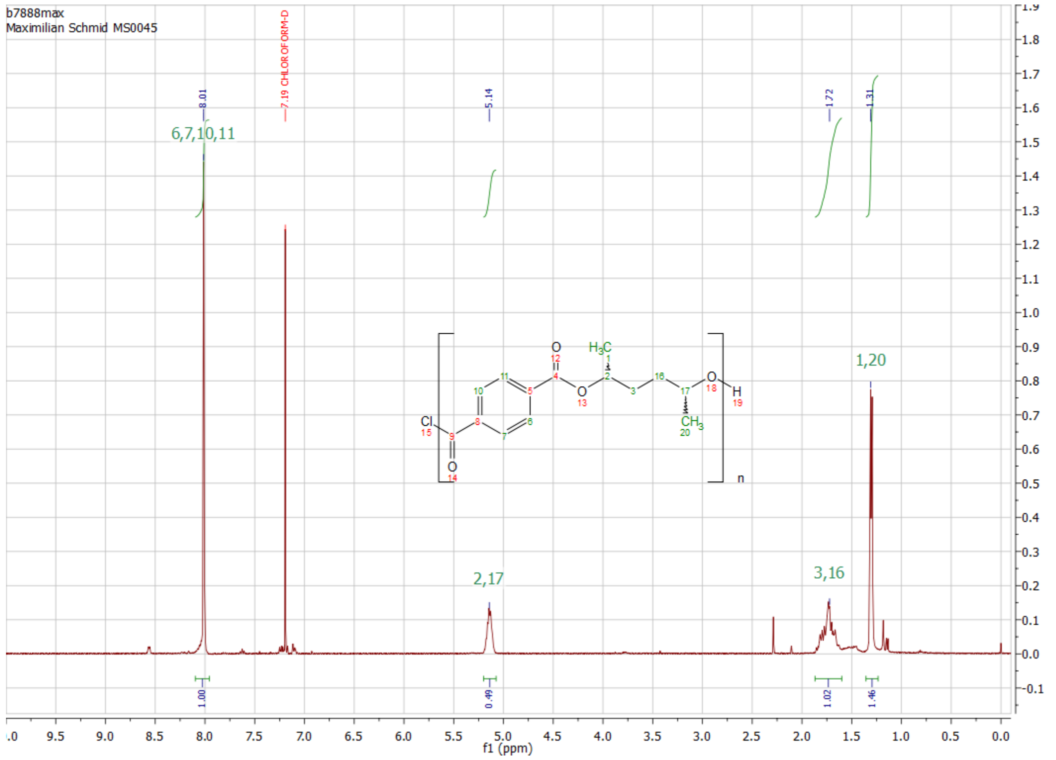

$CDCl_3$ solvent, 400 MHz, TMS reference, peak at ~1.7 ppm includes HOD as well as protons 3 and 16.

Figure S4c. ^{1}H NMR spectrum of P-**13-7**

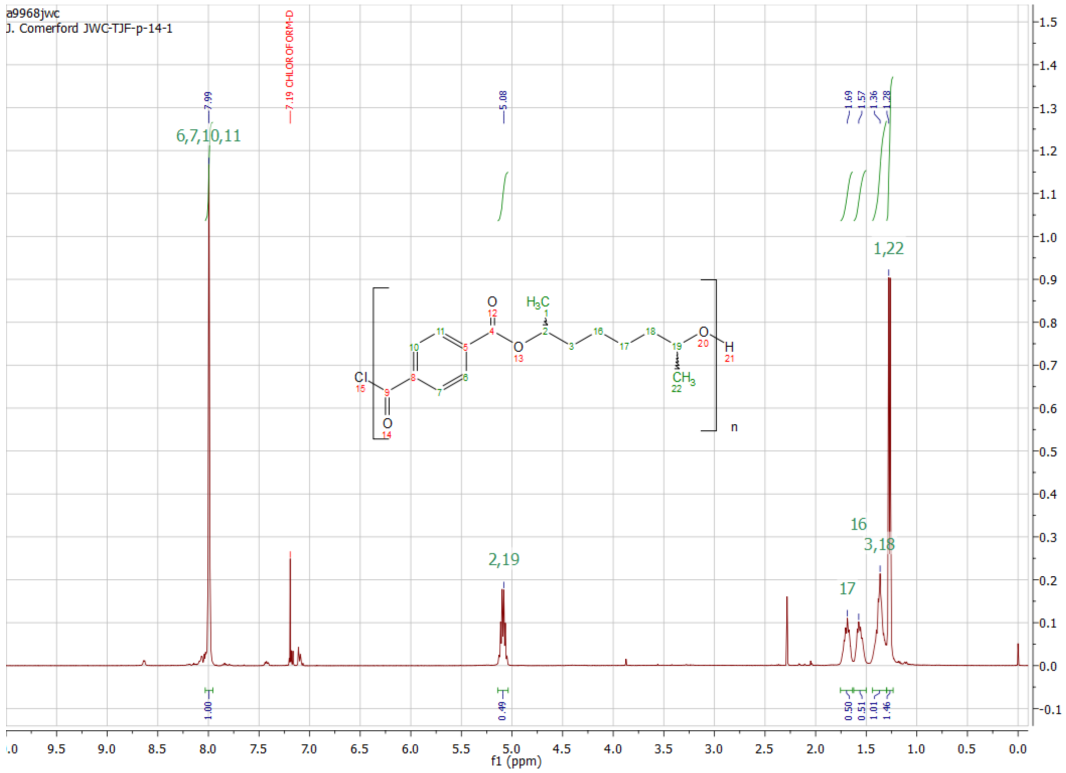

CDCl3 solvent, 400 MHz, TMS reference, peak at ~1.7 ppm includes HOD as well as protons 16 and 17.

Figure S4d. ^{1}H NMR spectrum of P-**13-15**

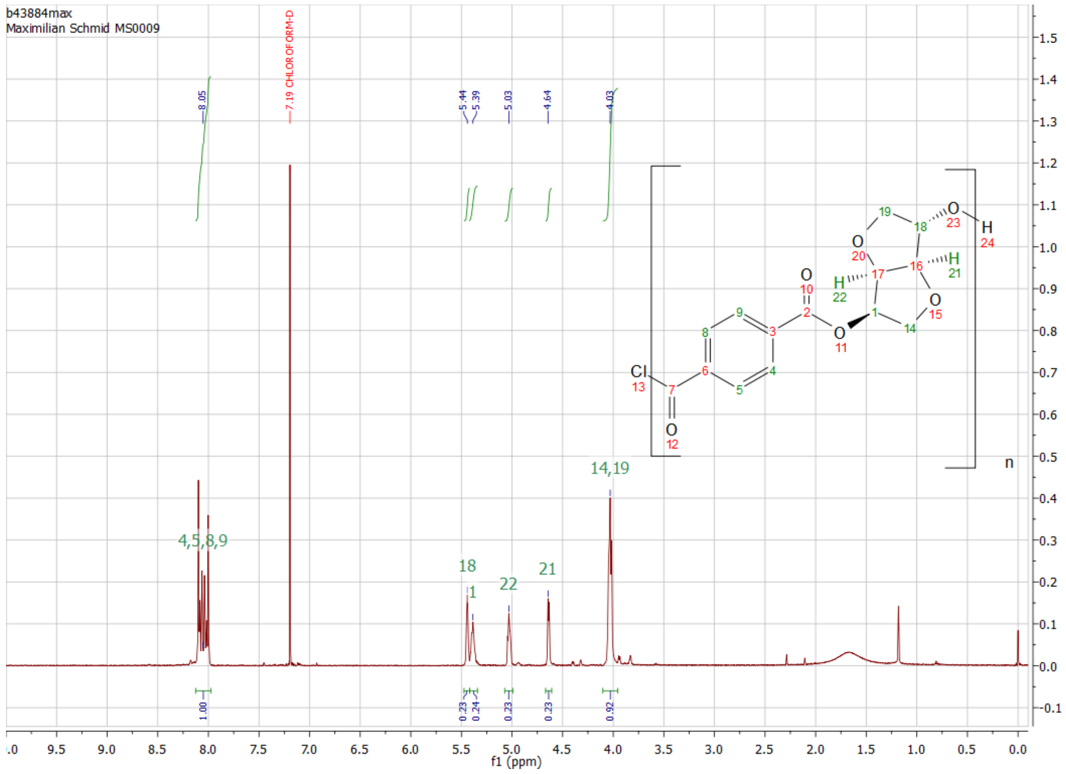

CDCl3 solvent, 400 MHz, TMS reference, peak at ~1.7 ppm includes HOD.

Figure S4e. ^{1}H NMR spectrum of P-**3-14**

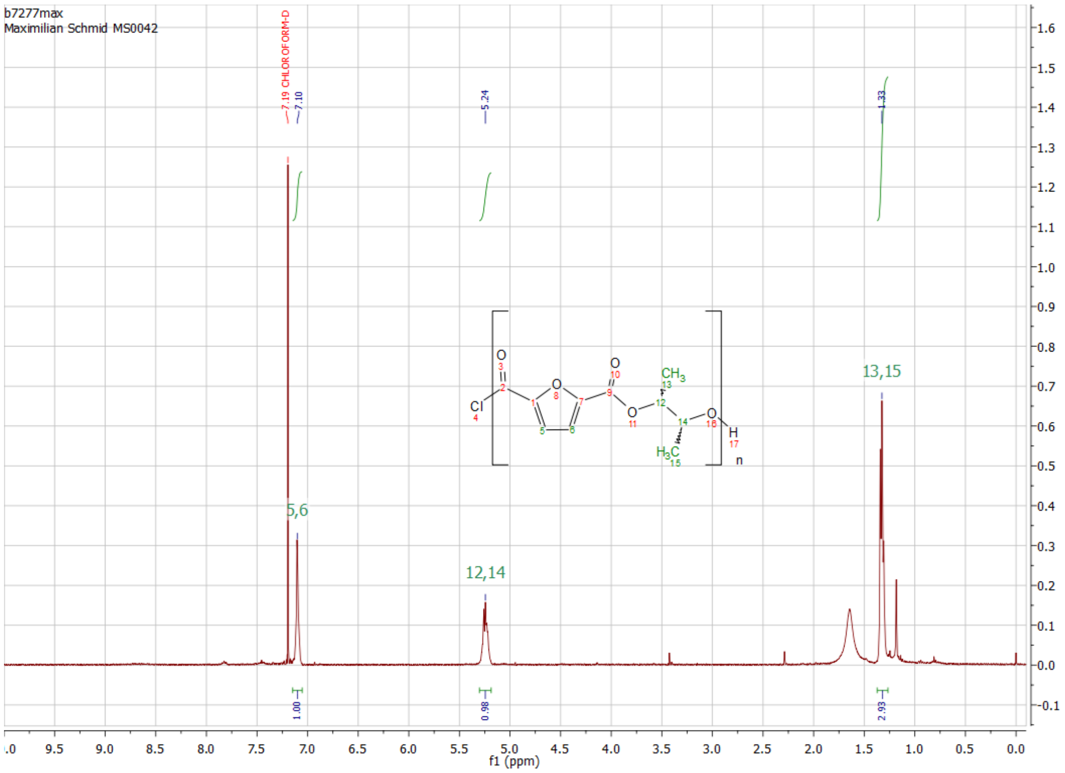

CDCl3 solvent, 400 MHz, TMS reference, peak at ~1.7 ppm includes HOD.

Figure S4f. ^{1}H NMR spectrum of P-**3-10**

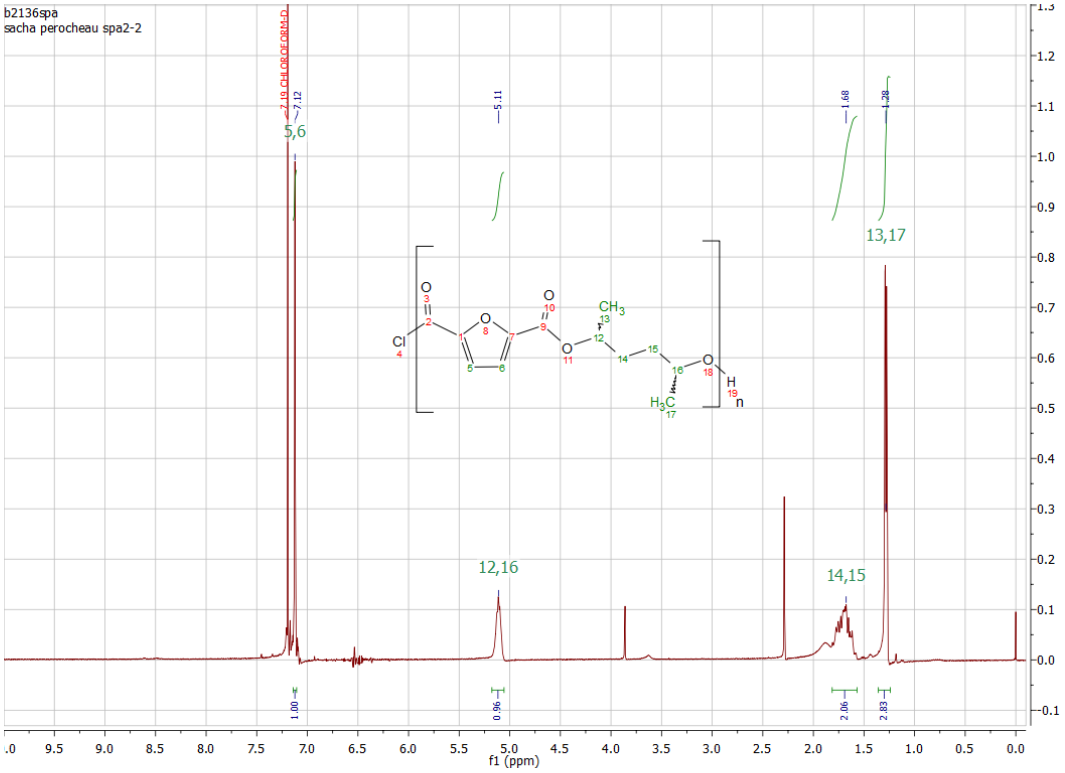

CDCl3 solvent, 400 MHz, TMS reference, peak at ~1.7 ppm includes HOD as well as protons 14 and 15.

Figure S4g. ^{1}H NMR spectrum of P-**3-7**

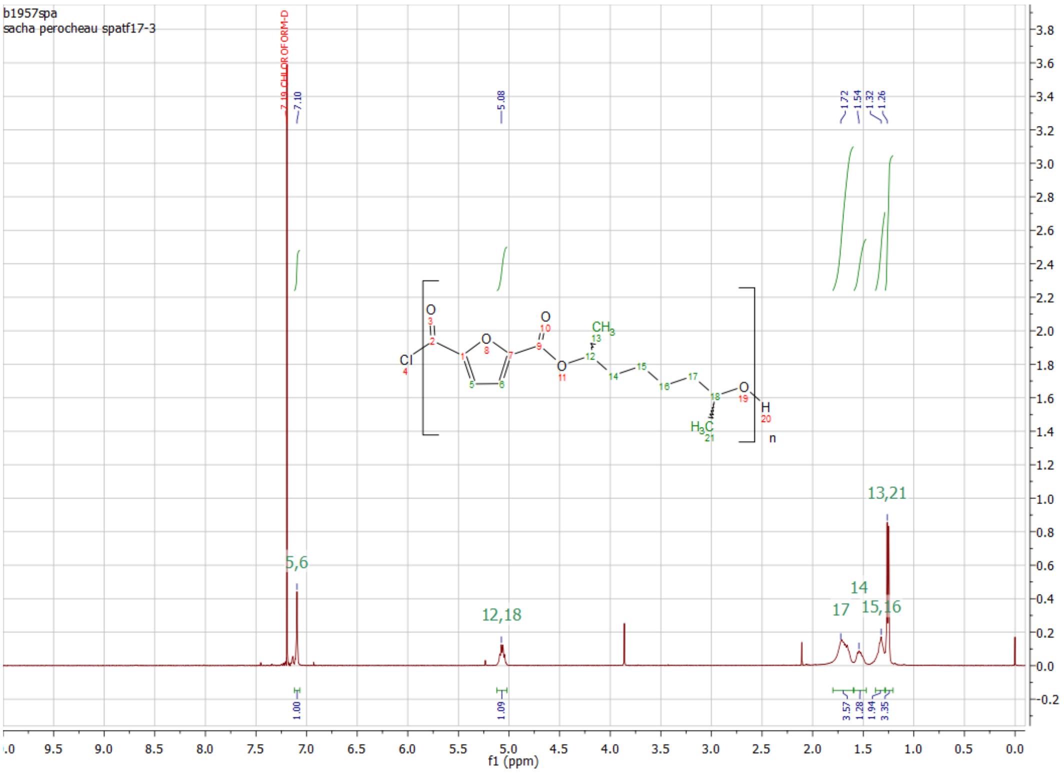

CDCl₃ solvent, 400 MHz, TMS reference, peak at ~1.7 ppm includes HOD as well as protons 17 and 14.

Figure S4h. ^{1}H NMR spectrum of P-**3-7** (24 hours)

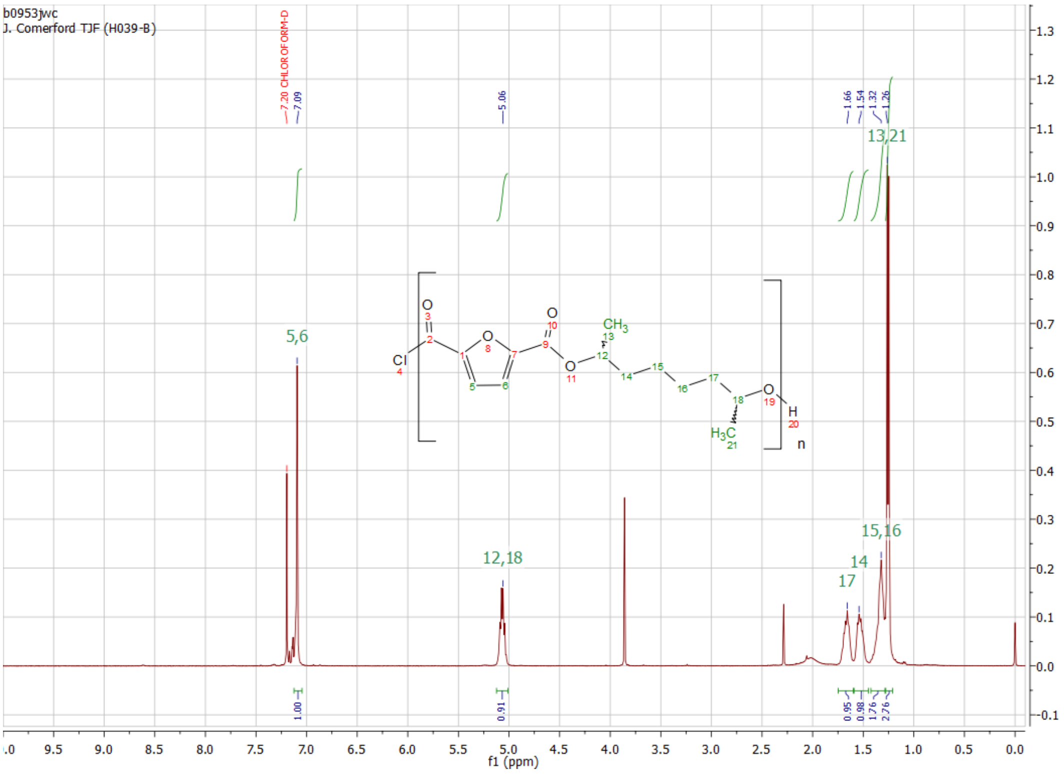

CDCl₃ solvent, 400 MHz, TMS reference

Figure S4i. ^{1}H NMR spectrum of P-**3-15**

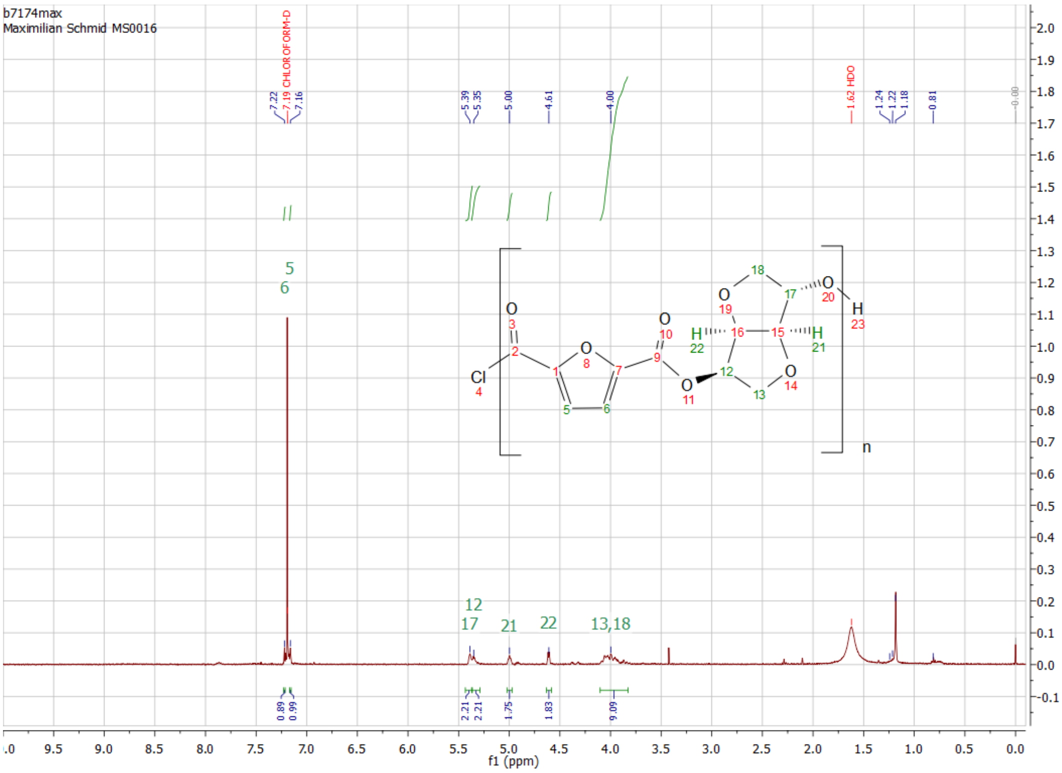

CDCl3 solvent, 400 MHz, TMS reference, peak at ~1.7 ppm includes HOD

Figure S4j. ^{1}H NMR spectrum of CP-**13-15-14**

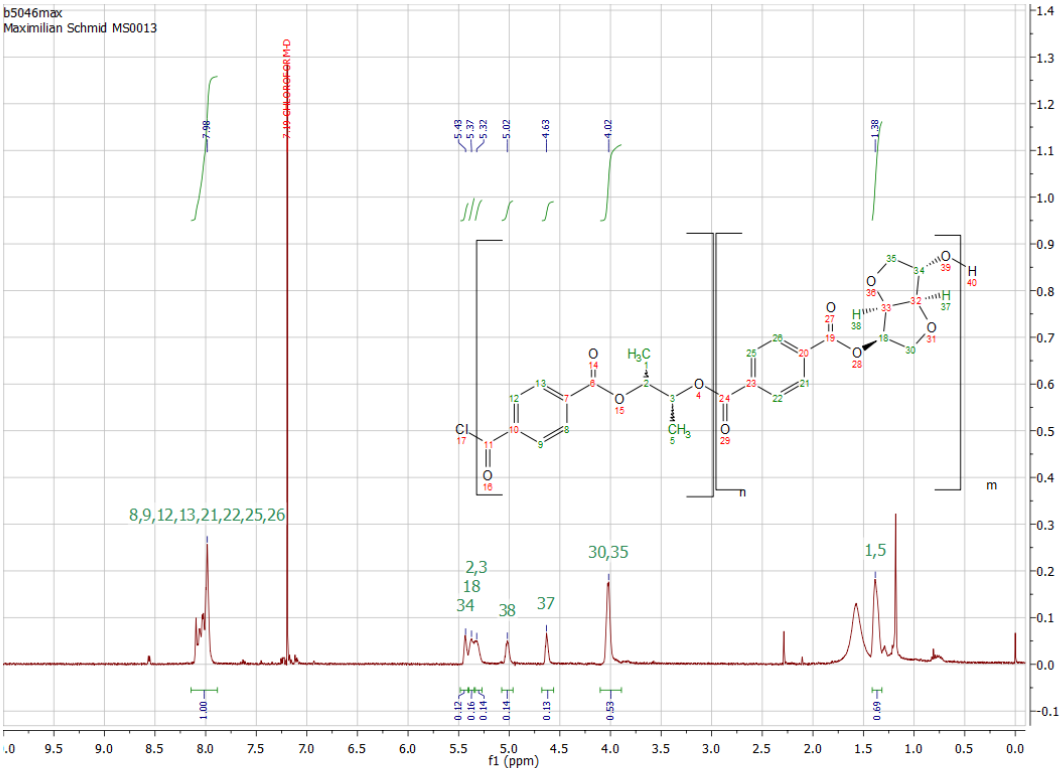

CDCl3 solvent, 400 MHz, TMS reference, peak at ~1.7 ppm includes HOD.

Figure S4k. ^{1}H NMR spectrum of CP-**13-15-10**

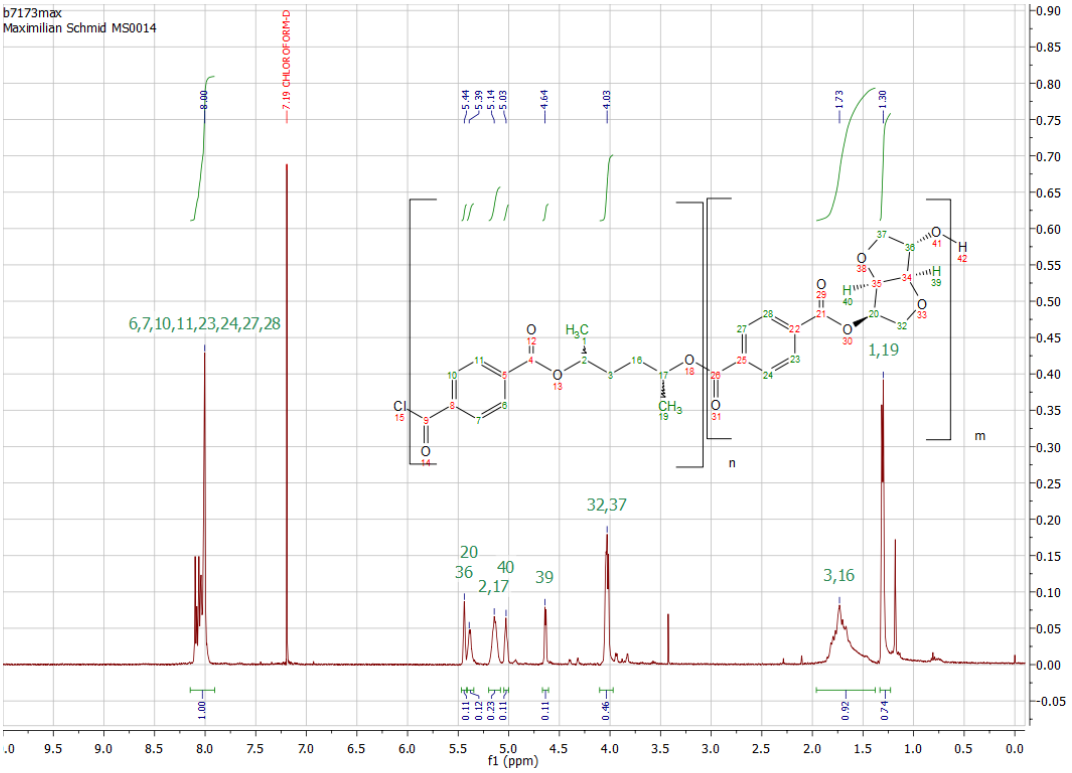

CDCl3 solvent, 400 MHz, TMS reference, peak at ~1.7 ppm includes HOD as well as protons 3 and 16.

Figure S4l. ^{1}H NMR spectrum of CP-**13-15-7**

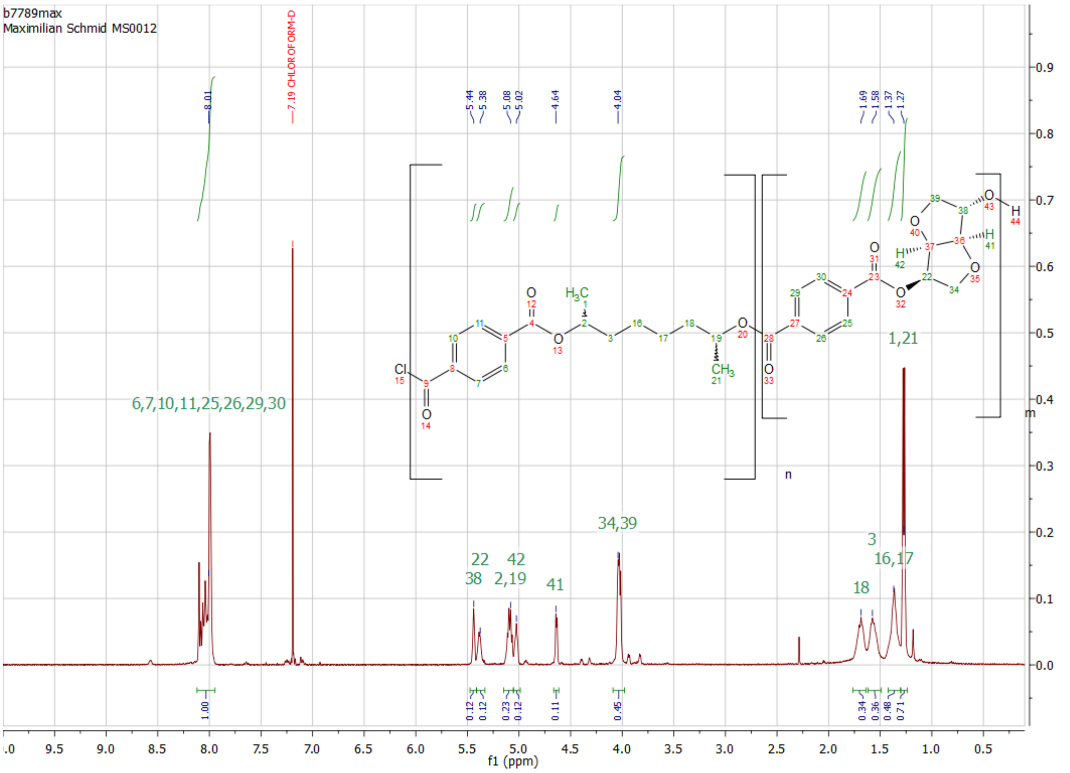

CDCl3 solvent, 400 MHz, TMS reference

Figure S4m. ^{1}H NMR spectrum of CP-**3-15-14**

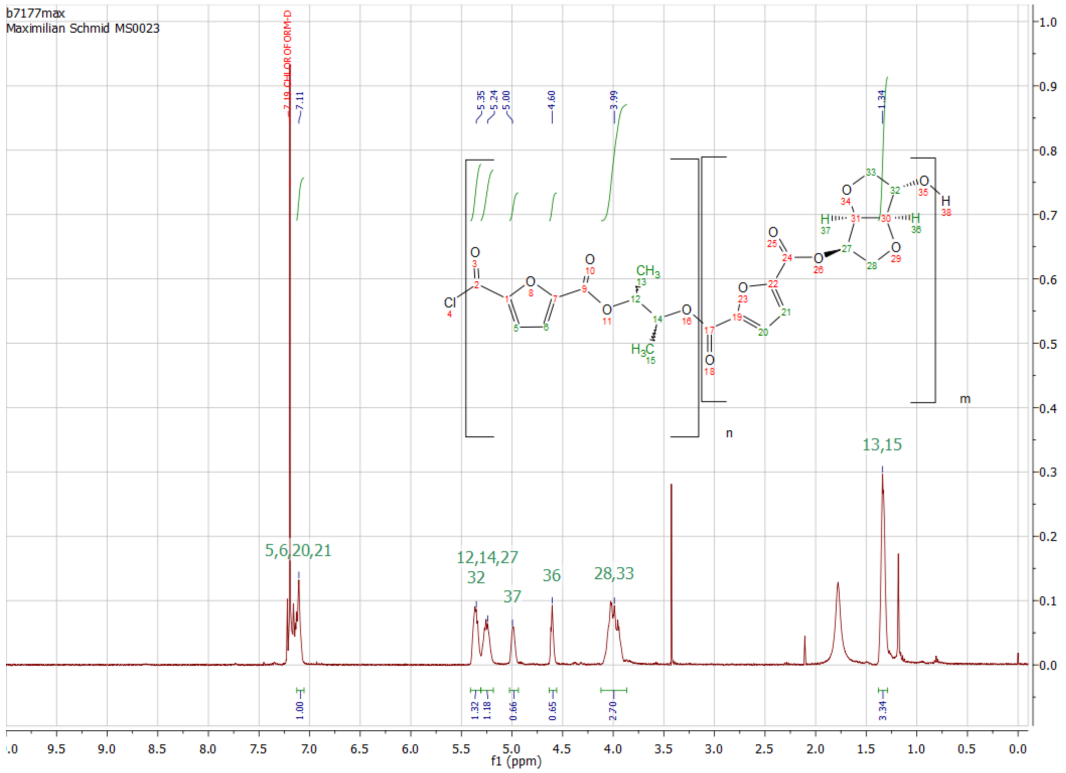

CDCl3 solvent, 400 MHz, TMS reference, peak at ~1.7 ppm includes HOD.

Figure S4n. ^{1}H NMR spectrum of CP-**3-15-10**

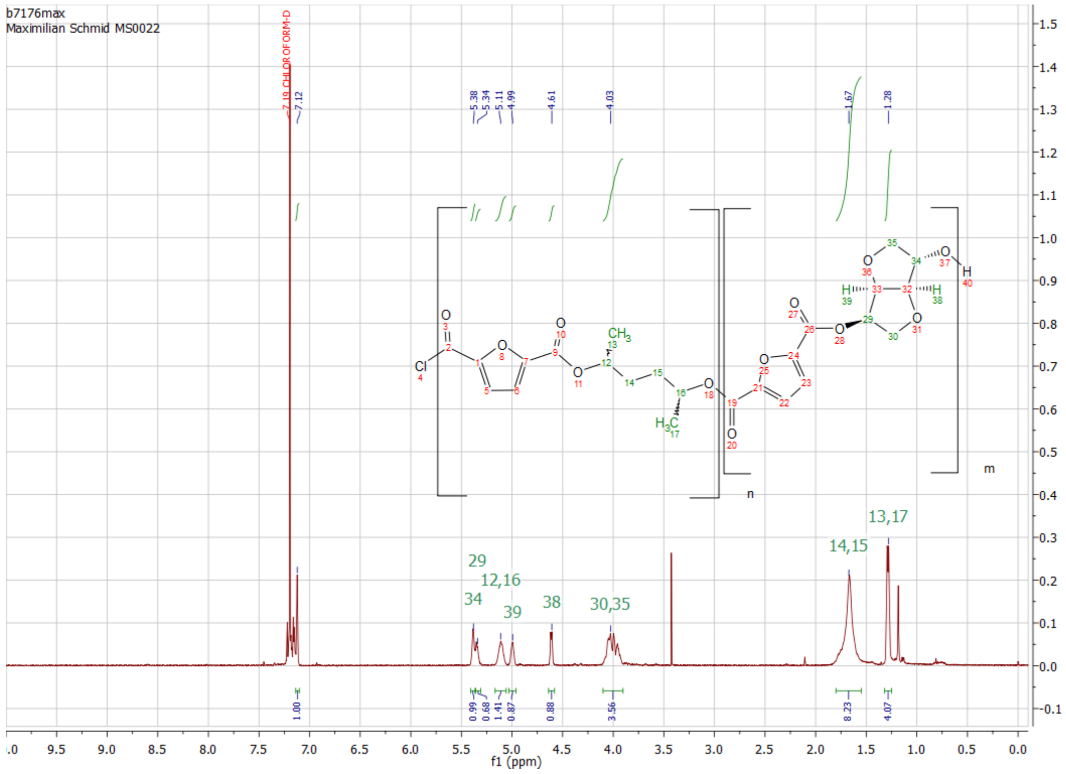

CDCl3 solvent, 400 MHz, TMS reference, peak at ~1.7 ppm includes HOD as well as protons 14 and 15.

Figure S4o. ^{1}H NMR spectrum of CP-**3-15-7**

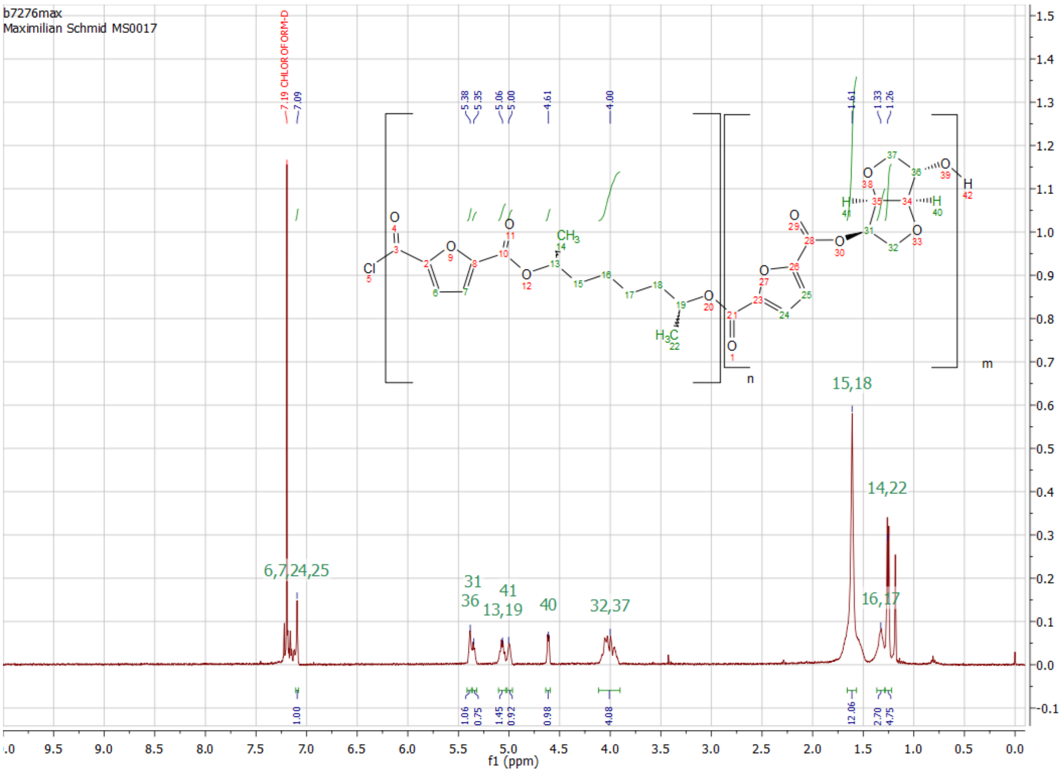

CDCl3 solvent, 400 MHz, TMS reference, peak at ~1.7 ppm includes HOD as well as protons 15 and 18.

Figure S4p. ^{1}H NMR spectrum of CP-**3-15-7**-25%iso

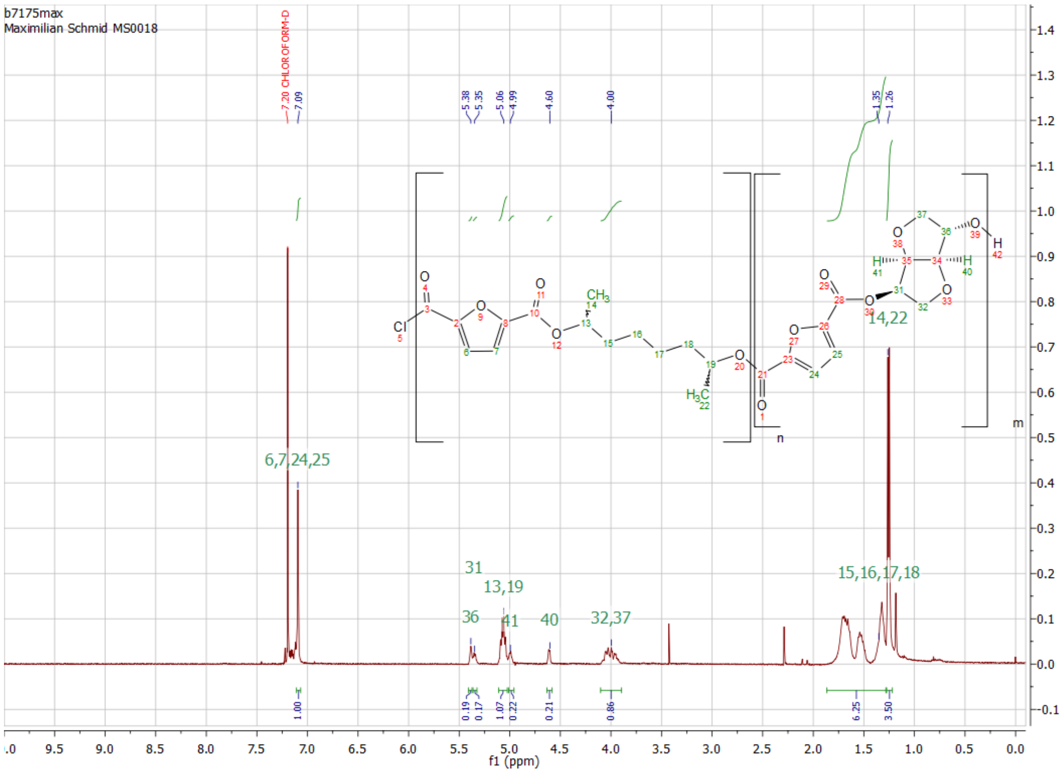

CDCl3 solvent, 400 MHz, TMS reference, peak at ~1.5 ppm includes HOD as well as protons 15-18.

Figure S4q. ^{1}H NMR spectrum of TP-**4a-14**

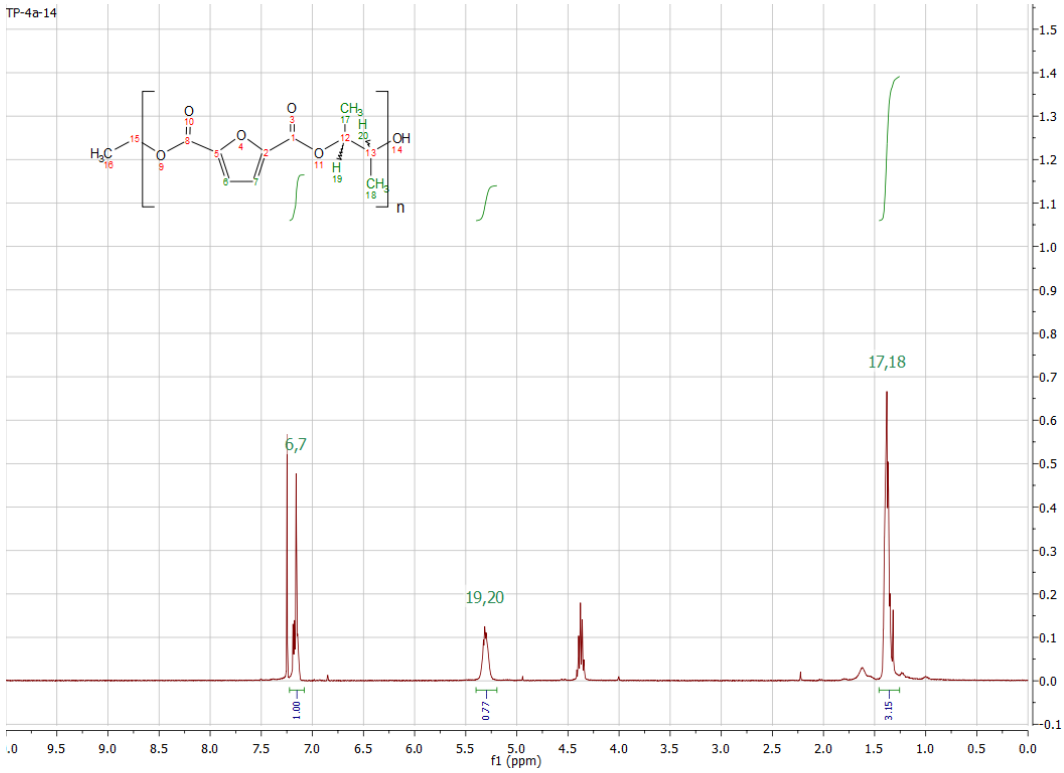

CDCl3 solvent, 400 MHz, TMS reference, peak at ~1.7 ppm includes HOD.

Figure S4r. ^{1}H NMR spectrum of TP-**4a-10**

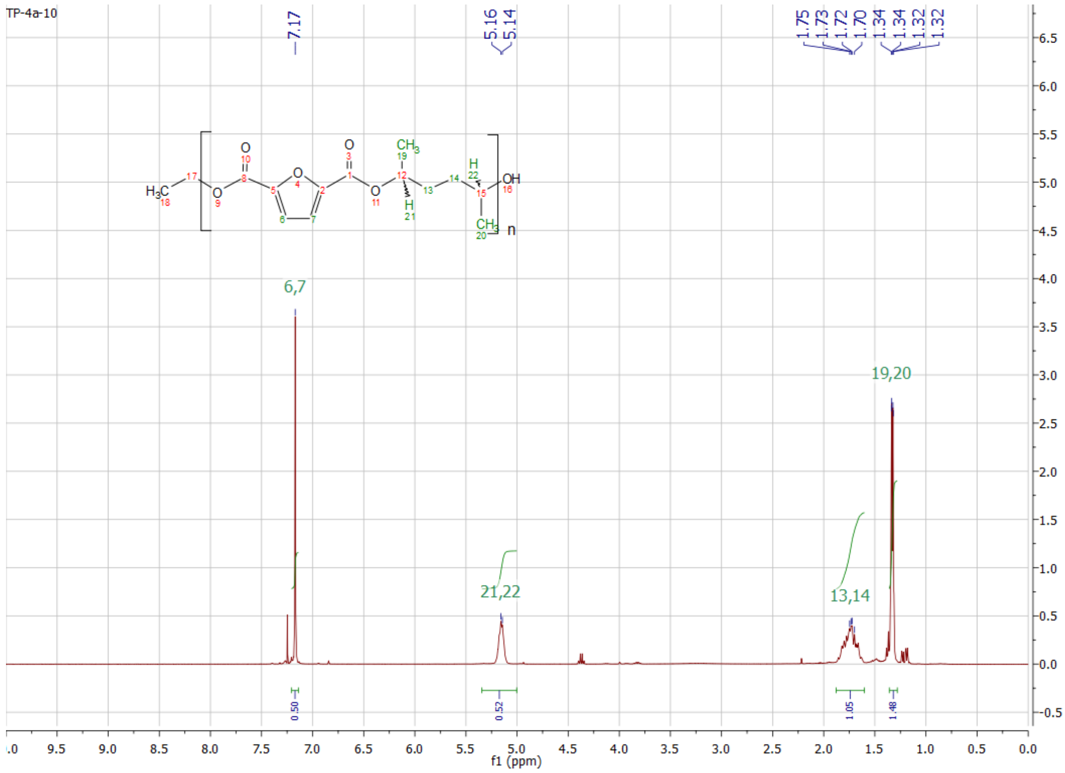

CDCl3 solvent, 400 MHz, TMS reference, peak at ~1.7 ppm includes HOD as well as protons 13 and 14.

Figure S4s. ^{1}H NMR spectrum of TP-**4a-7**

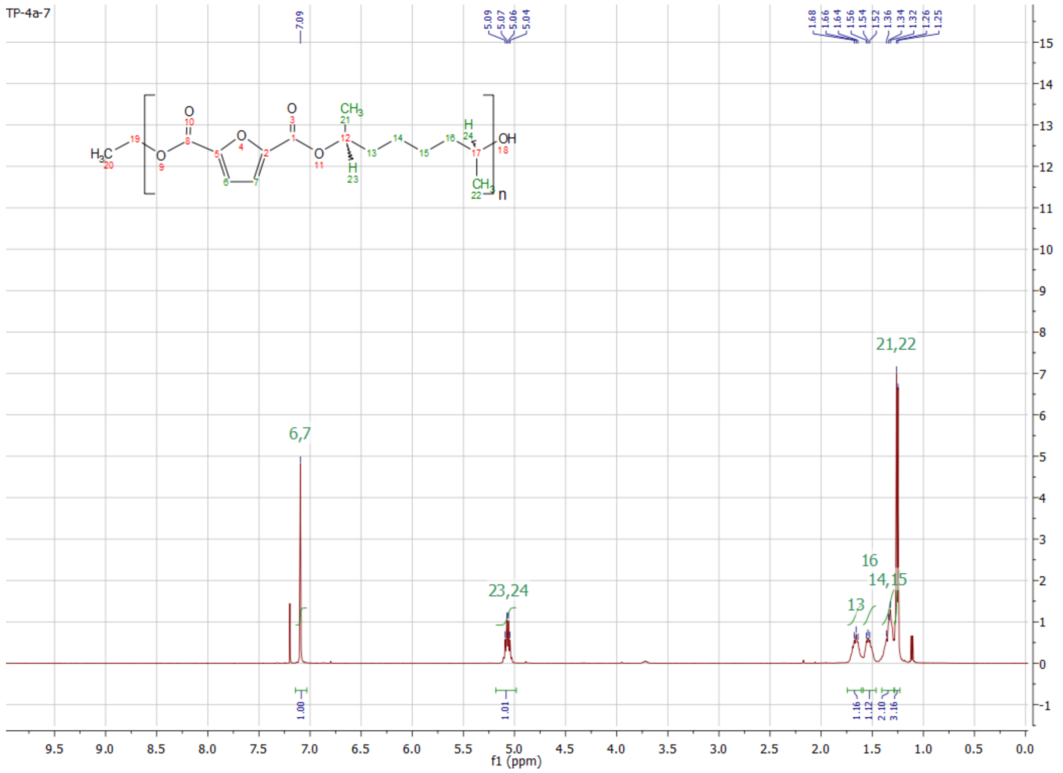

CDCl3 solvent, 400 MHz, TMS reference.

Figure S4t. ^{1}H NMR spectrum of TP-**17-14**

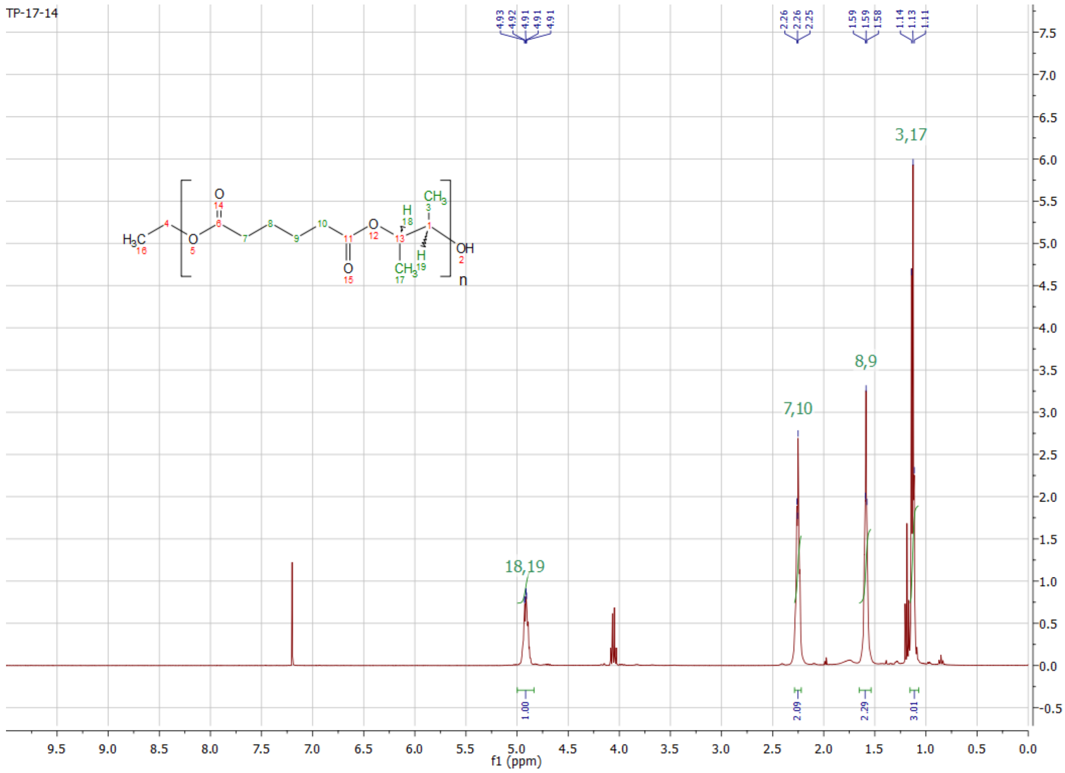

CDCl3 solvent, 400 MHz, TMS reference, peak at ~1.7 ppm includes HOD.

Figure S4u. ^{1}H NMR spectrum of TP-**17-10**

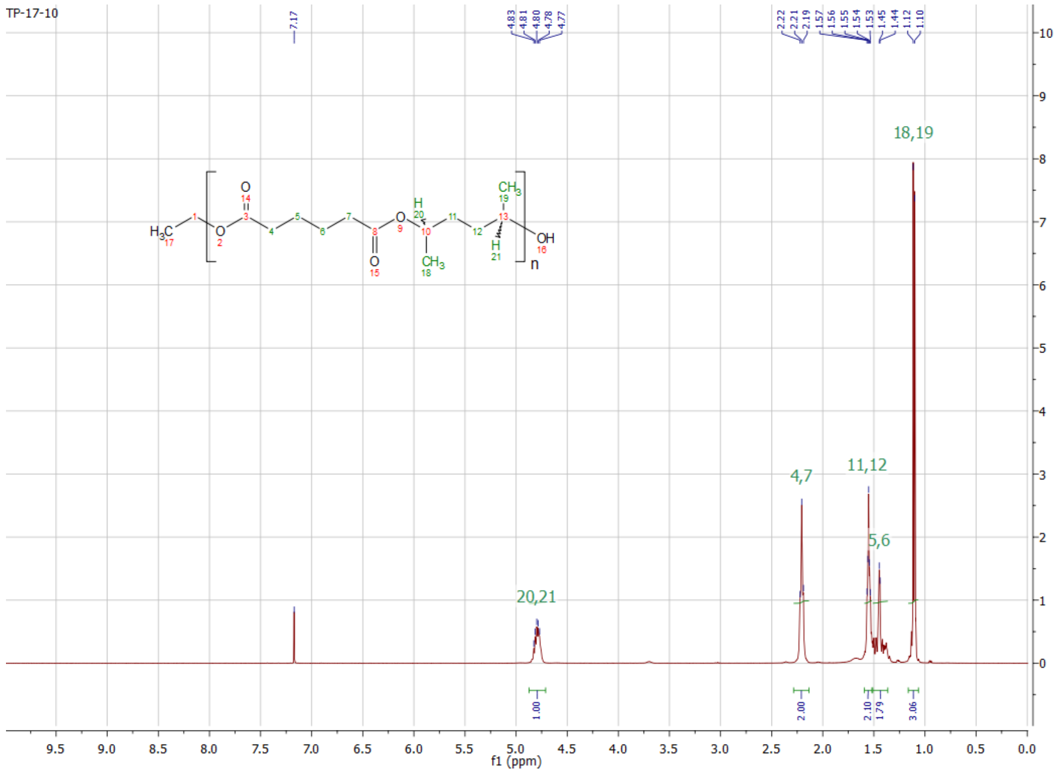

$CDCl_3$ solvent, 400 MHz, TMS reference, peak at ~1.7 ppm includes HOD.

Figure S4v. ^{1}H NMR spectrum of TP-**17-7**

$CDCl_3$ solvent, 400 MHz, TMS reference

Figure S4w. ^{1}H NMR spectrum of TCP-**4a-17-10**

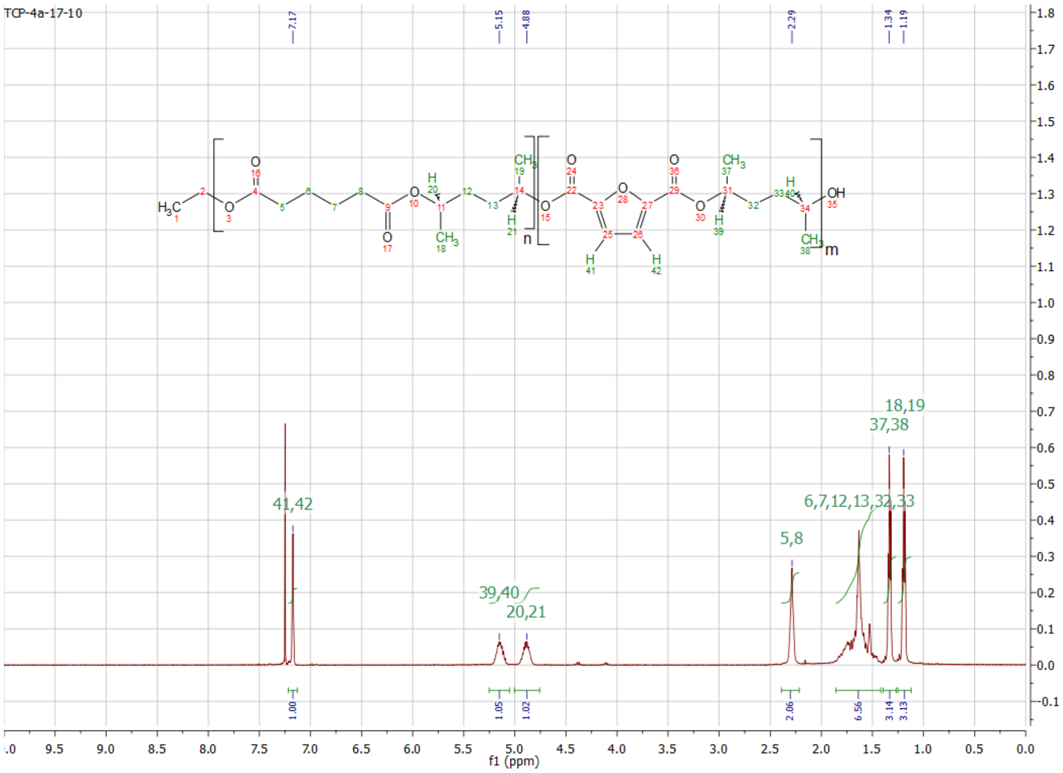

CDCl3 solvent, 400 MHz, TMS reference, peak at ~1.7 ppm includes HOD as well as protons 6, 7, 12, 13, 32 and 33.

Figure S4x. ^{1}H NMR spectrum of TCP-**4a-17-7**

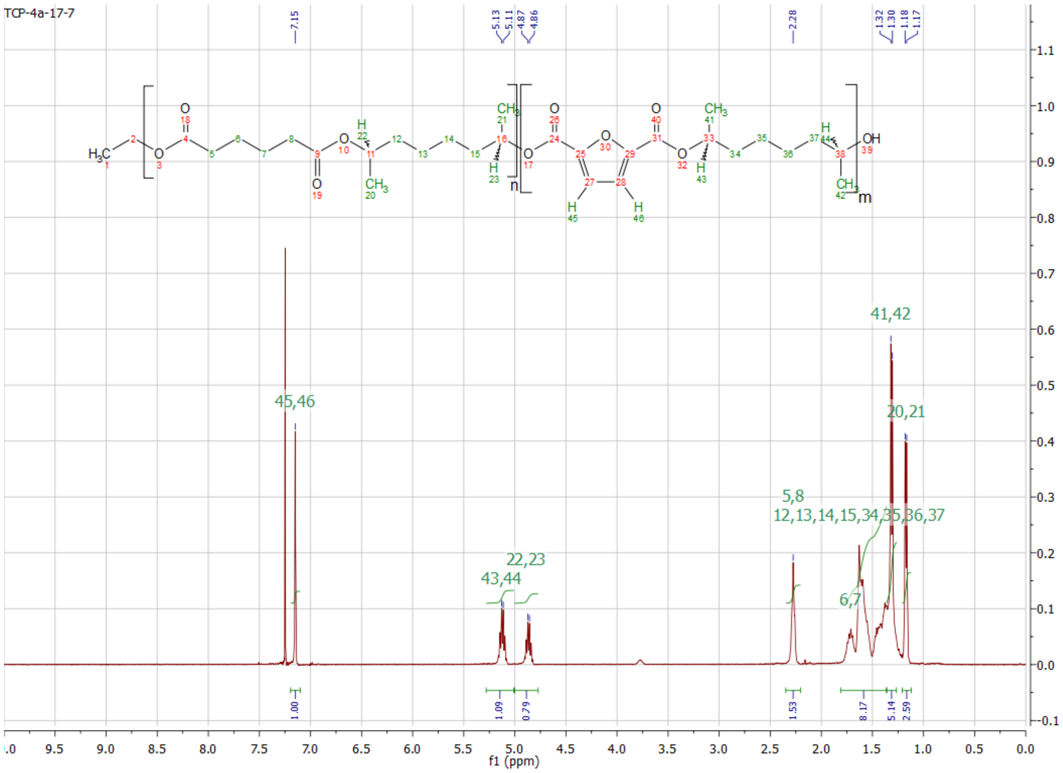

CDCl3 solvent, 400 MHz, TMS reference

Thermo-gravimetric traces of polymers

Figure S5a. Thermo-gravimetric analysis of P-**13-14**

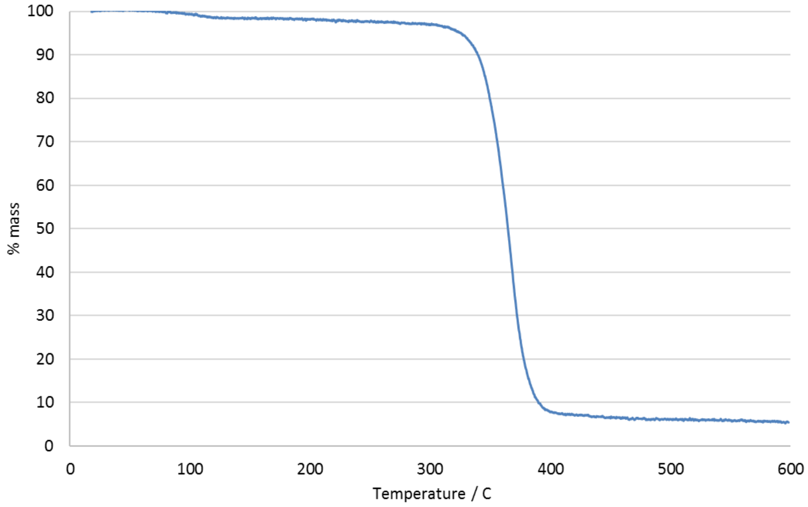

Figure S5b. Thermo-gravimetric analysis of P-**13-10**

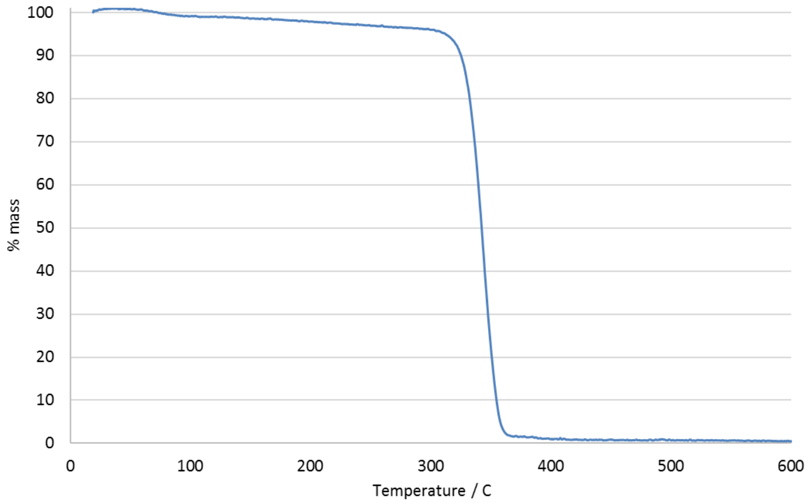

Figure S5c. Thermo-gravimetric analysis of P-**13-7**

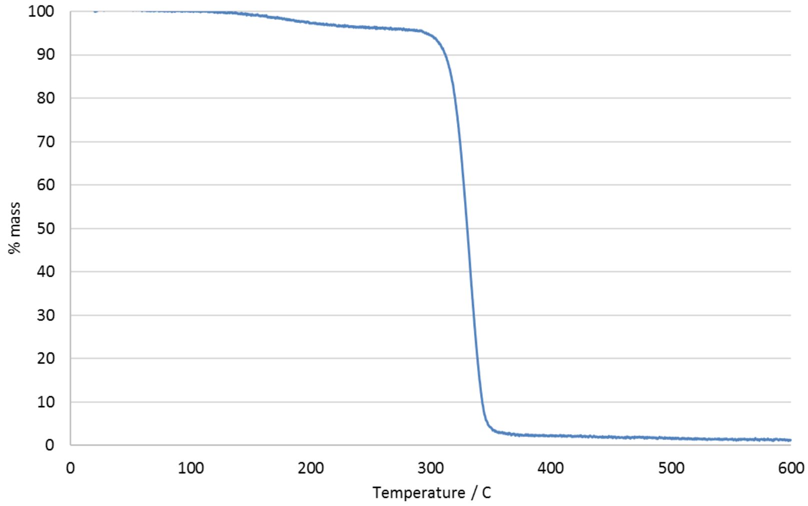

Figure S5d. Thermo-gravimetric analysis of P-**13-15**

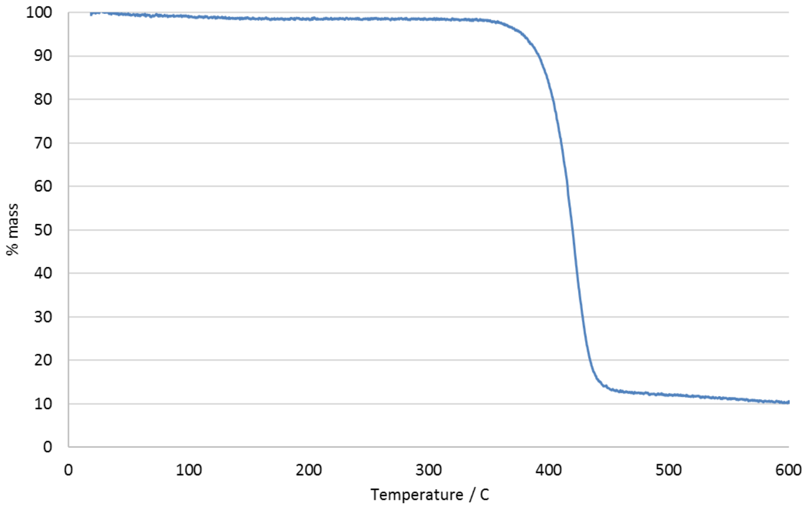

Figure S5e. Thermo-gravimetric analysis of P-**3-14**

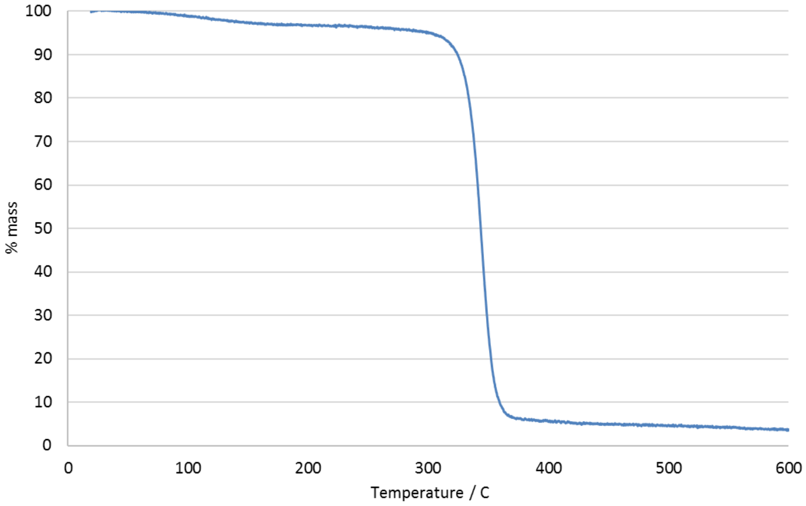

Figure S5f. Thermo-gravimetric analysis of P-**3-10**

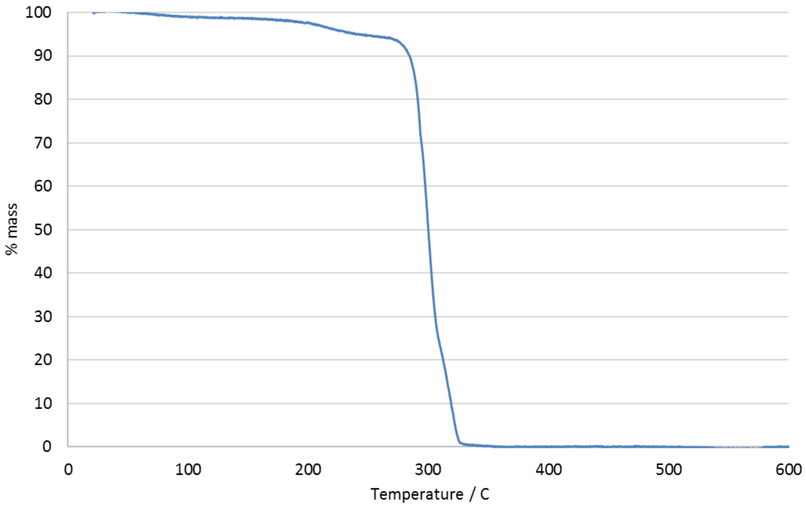

Figure S5g. Thermo-gravimetric analysis of P-**3-7**

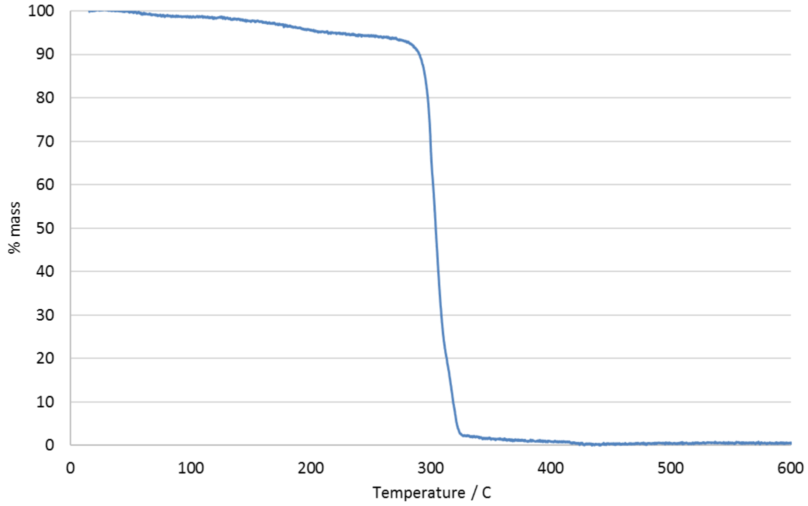

Figure S5h. Thermo-gravimetric analysis of P-**3-7**-24h

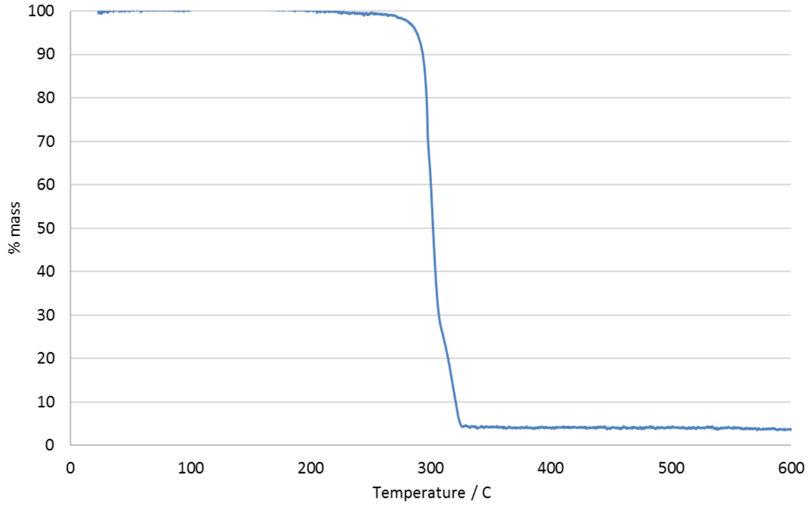

Figure S5i. Thermo-gravimetric analysis of P-**3-15**

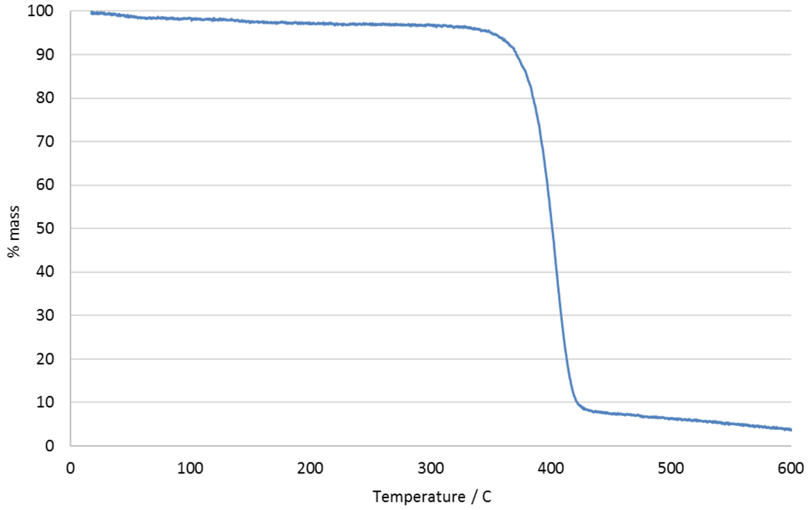

Figure S5j. Thermo-gravimetric analysis of CP-**13-15-14**

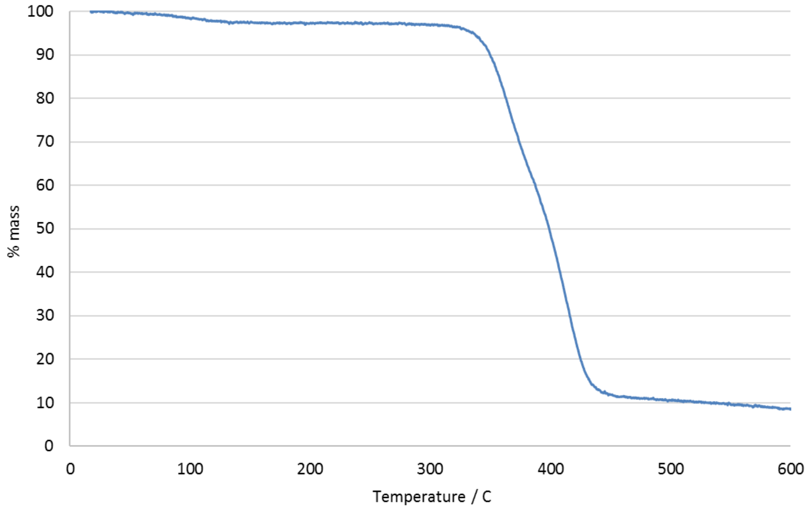

Figure S5k. Thermo-gravimetric analysis of CP-**13-15-10**

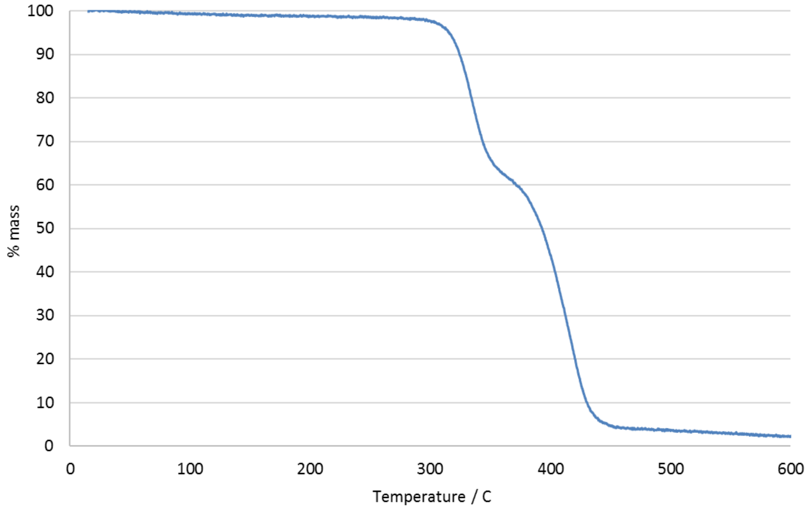

Figure S5l. Thermo-gravimetric analysis of CP-**13-15-7**

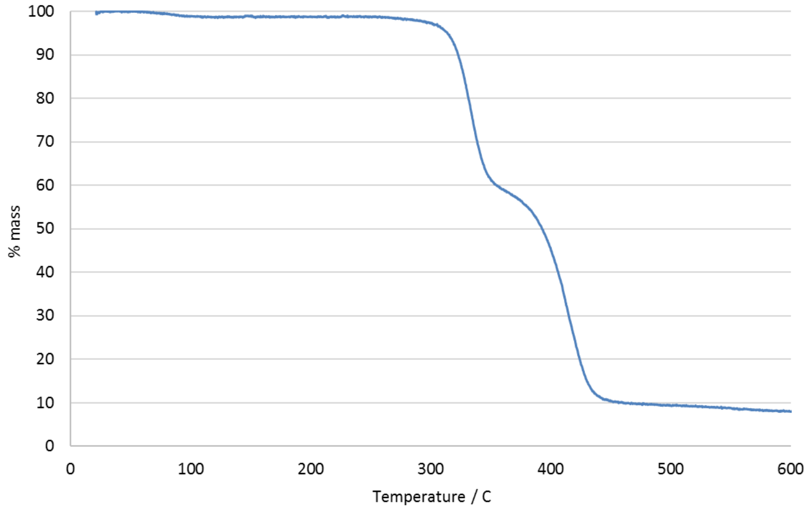

Figure S5m. Thermo-gravimetric analysis of CP-**3-15-14**

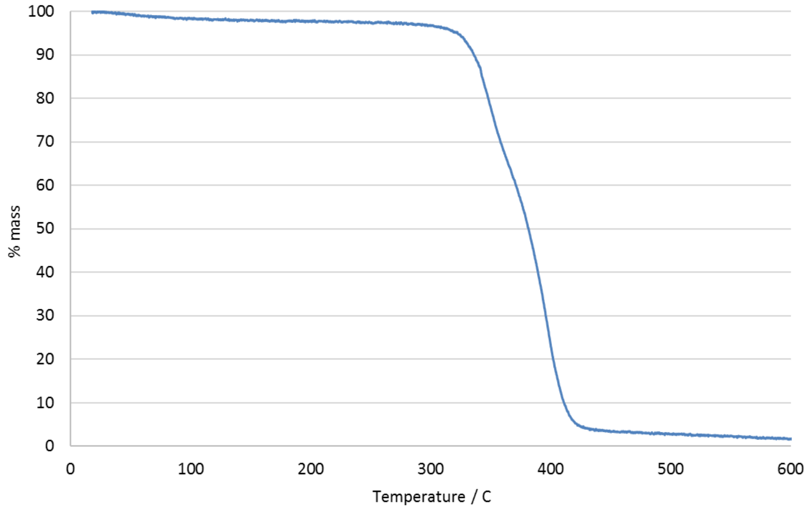

Figure S5n. Thermo-gravimetric analysis of CP-**3-15-10**

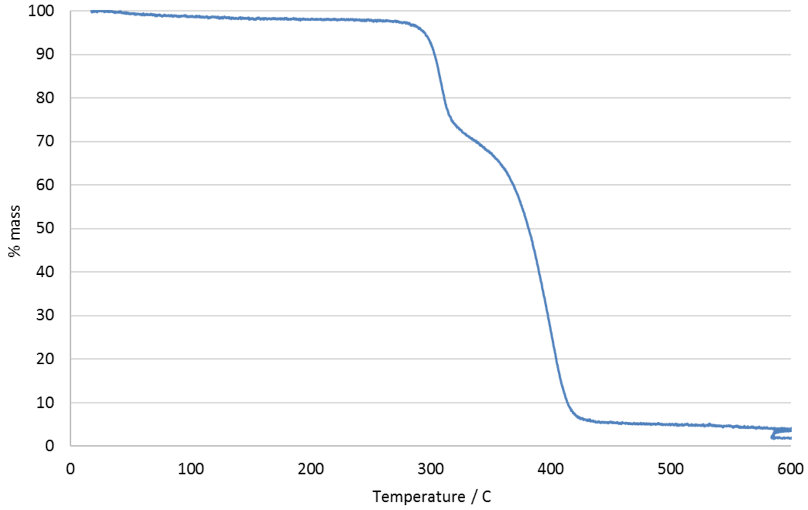

Figure S5o. Thermo-gravimetric analysis of CP-**3-15-7**

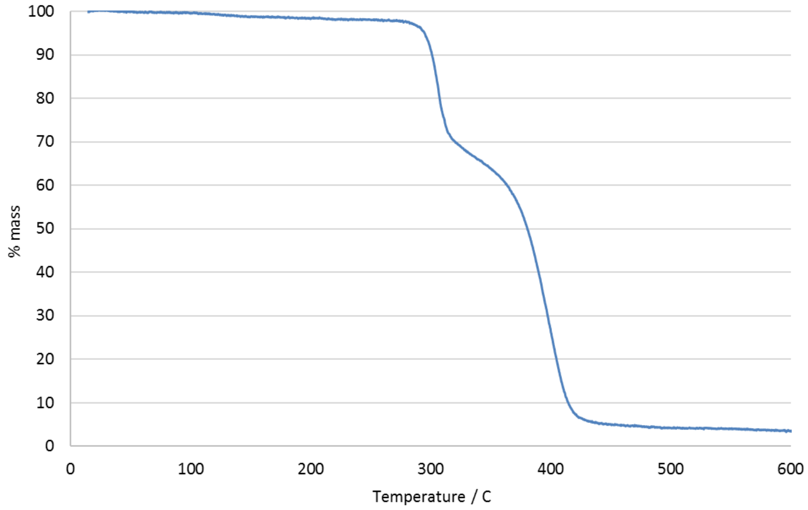

Figure S5p. Thermo-gravimetric analysis of CP-**3-15-7**-25%iso

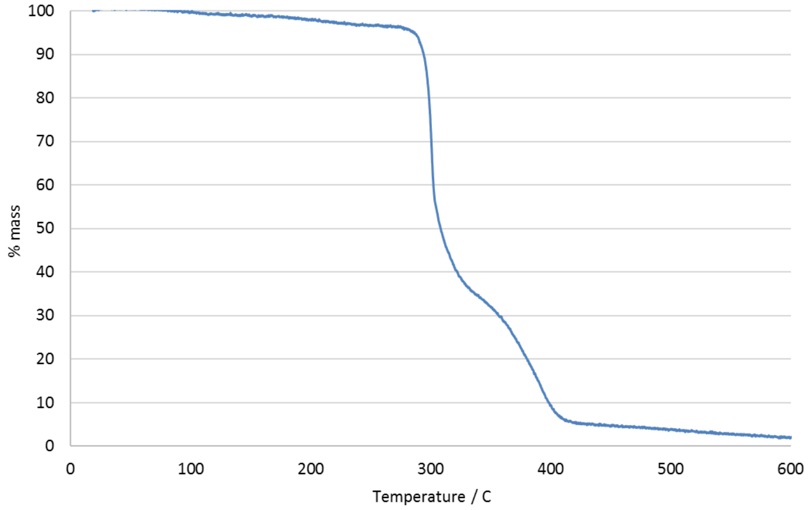

Modulated differential scanning calorimetry traces of polymers

Figure S6a. Modulated differential scanning calorimetry analysis of P-**13-14**

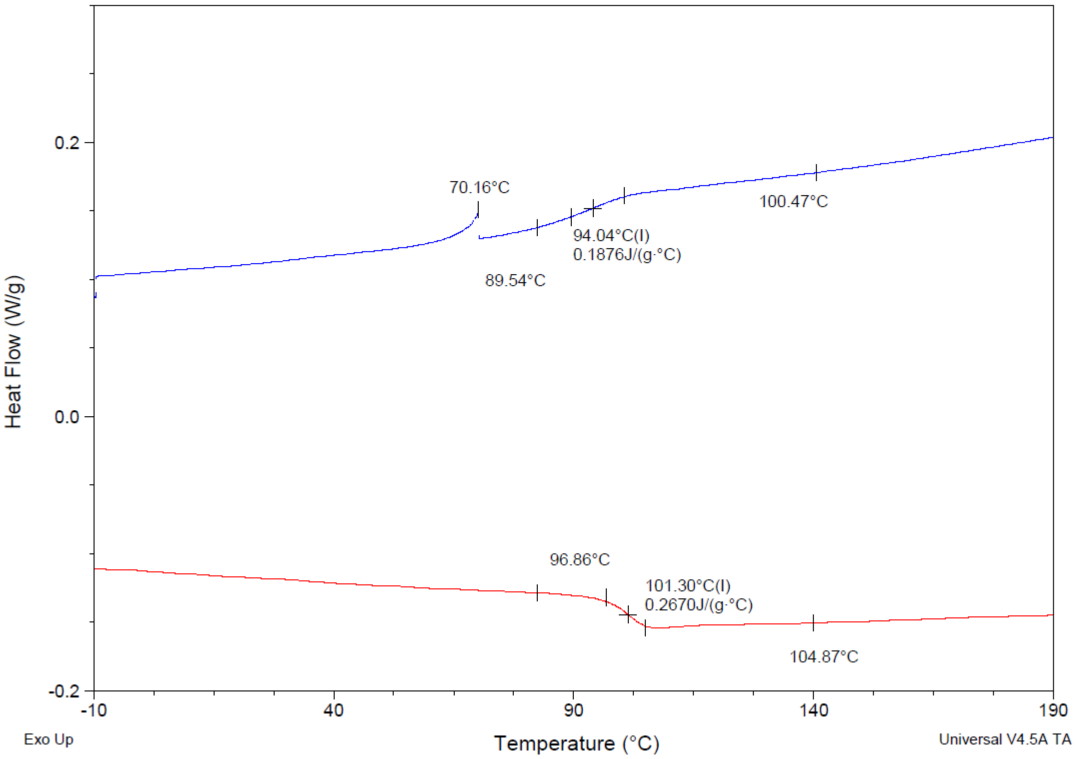

Heat-cool-heat-cool-heat over a -60 to 200 °C temperature range (10 °C/min), only final cool-heat cycle shown over the range -10 to 190 °C. Peak at 70.2 °C in the cool cycle is an artefact of the chiller unit and not related to the sample.

Figure S6b. Modulated differential scanning calorimetry analysis of P-**13-10**

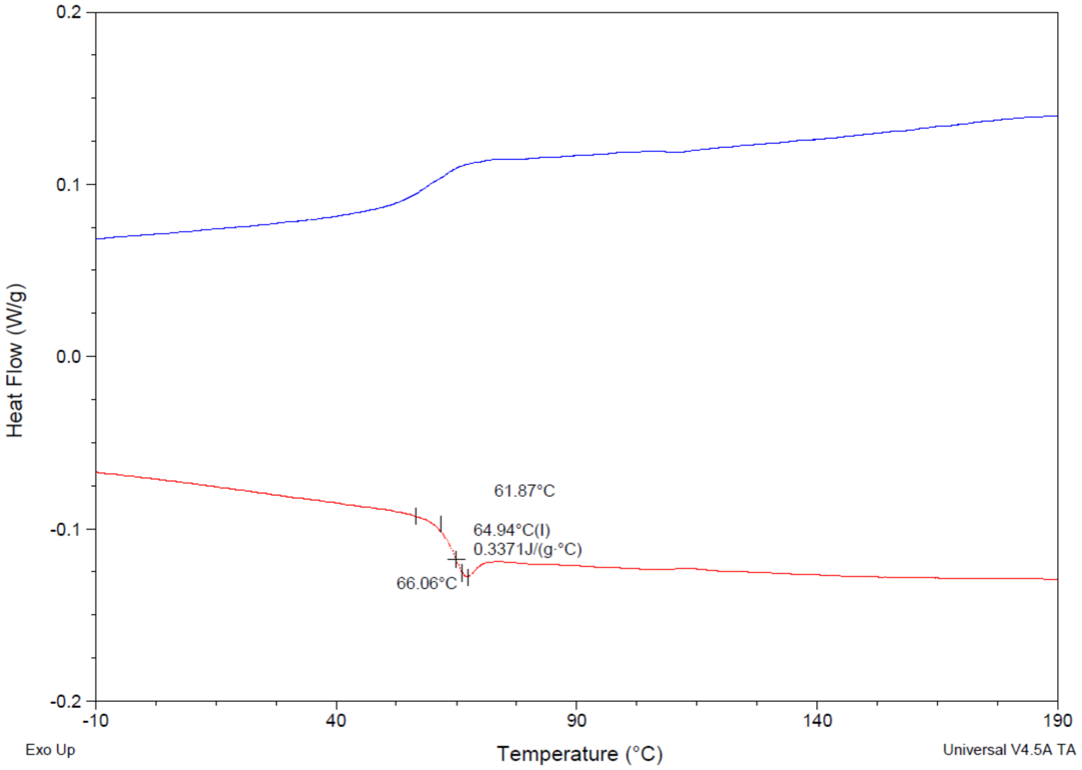

Heat-cool-heat-cool-heat over a -60 to 200 °C temperature range (10 °C/min), only final cool-heat cycle shown over the range -10 to 190 °C.

Figure S6c. Modulated differential scanning calorimetry analysis of P-**13-7**

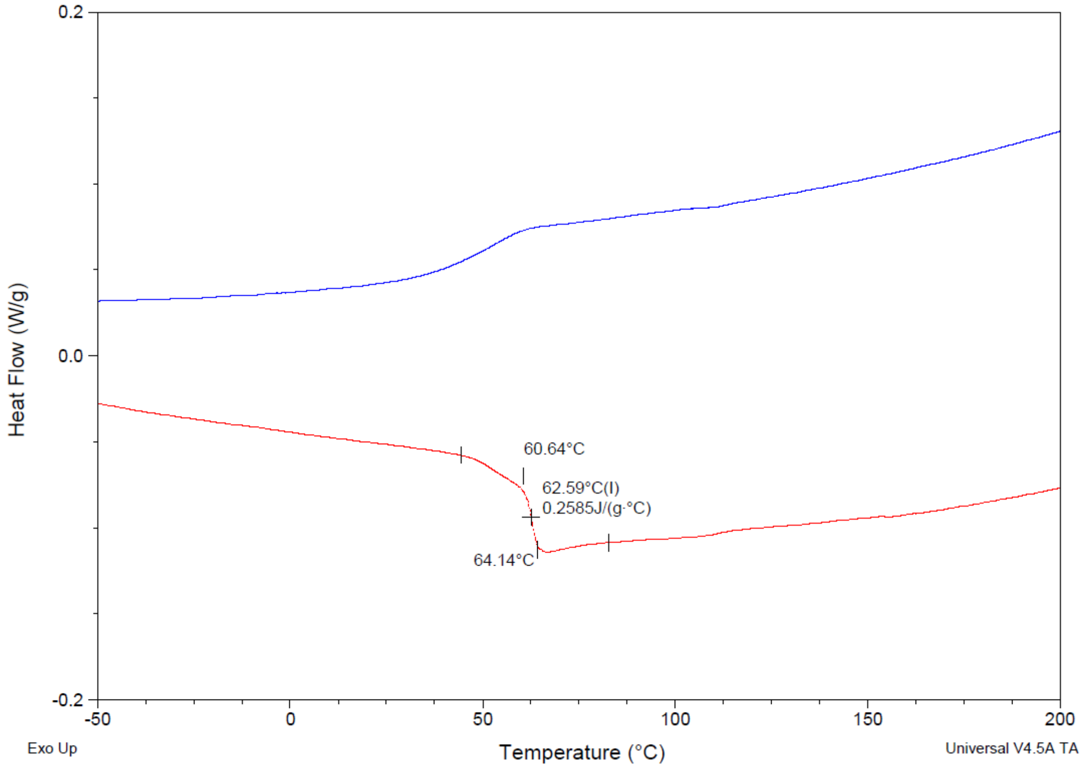

Heat-cool-heat-cool-heat over a -60 to 200 °C temperature range (10 °C/min), only final cool-heat cycle shown over the range -10 to 190 °C.

Figure S6d. Modulated differential scanning calorimetry analysis of P-**13-15**

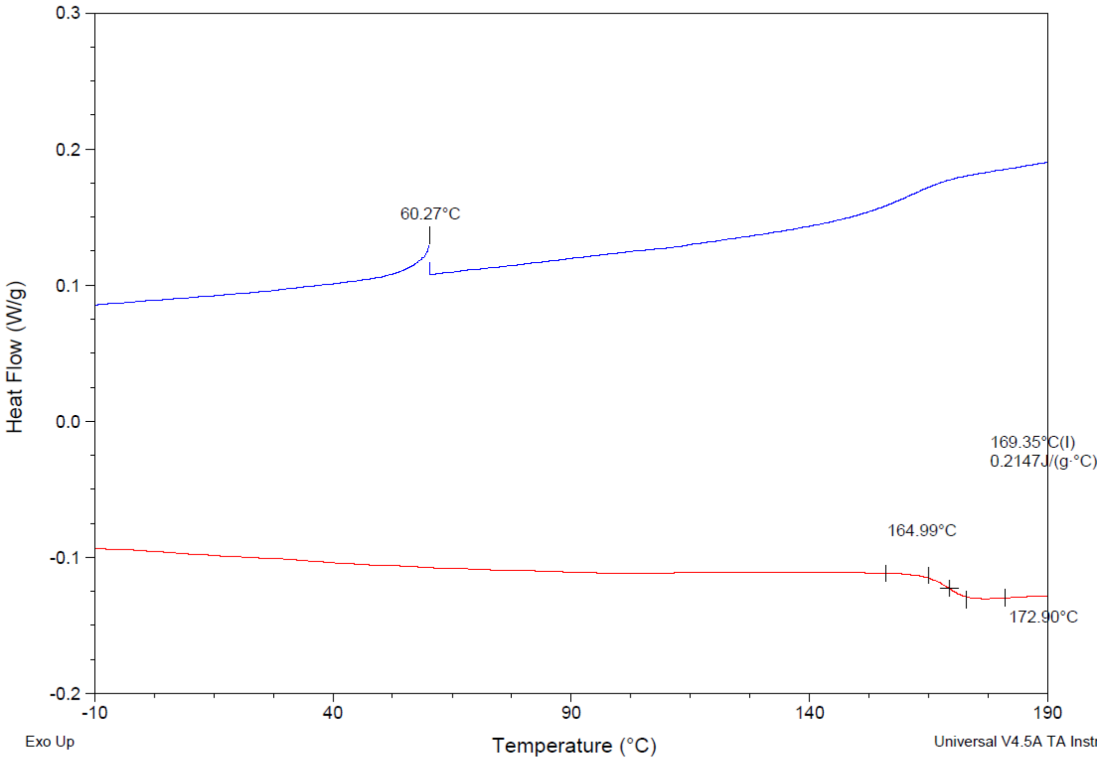

Heat-cool-heat-cool-heat over a -60 to 200 °C temperature range (10 °C/min), only final cool-heat cycle shown over the range -10 to 190 °C. Peak at 60.3 °C in the cool cycle is an artefact of the chiller unit and not related to the sample.

Figure S6e. Modulated differential scanning calorimetry analysis of P-**3-14**

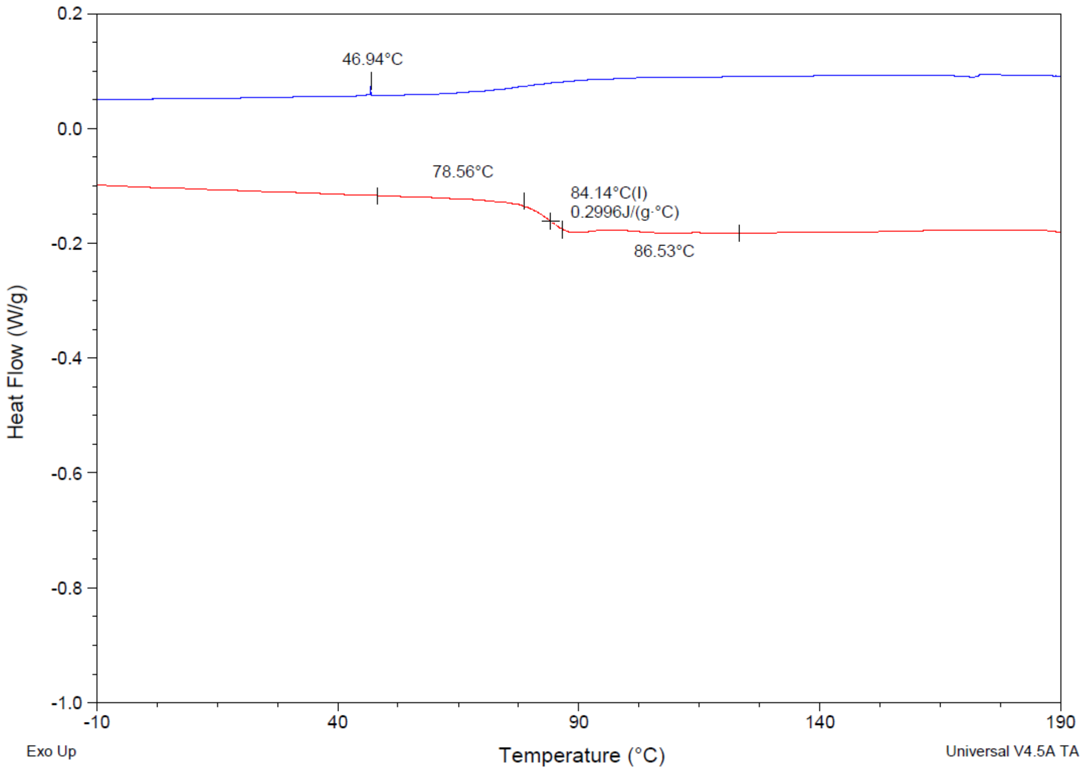

Heat-cool-heat-cool-heat over a -60 to 200 °C temperature range (10 °C/min), only final cool-heat cycle shown over the range -10 to 190 °C. Peak at 46.9 °C in the cool cycle is an artefact of the chiller unit and not related to the sample.

Figure S6f. Modulated differential scanning calorimetry analysis of P-**3-10**

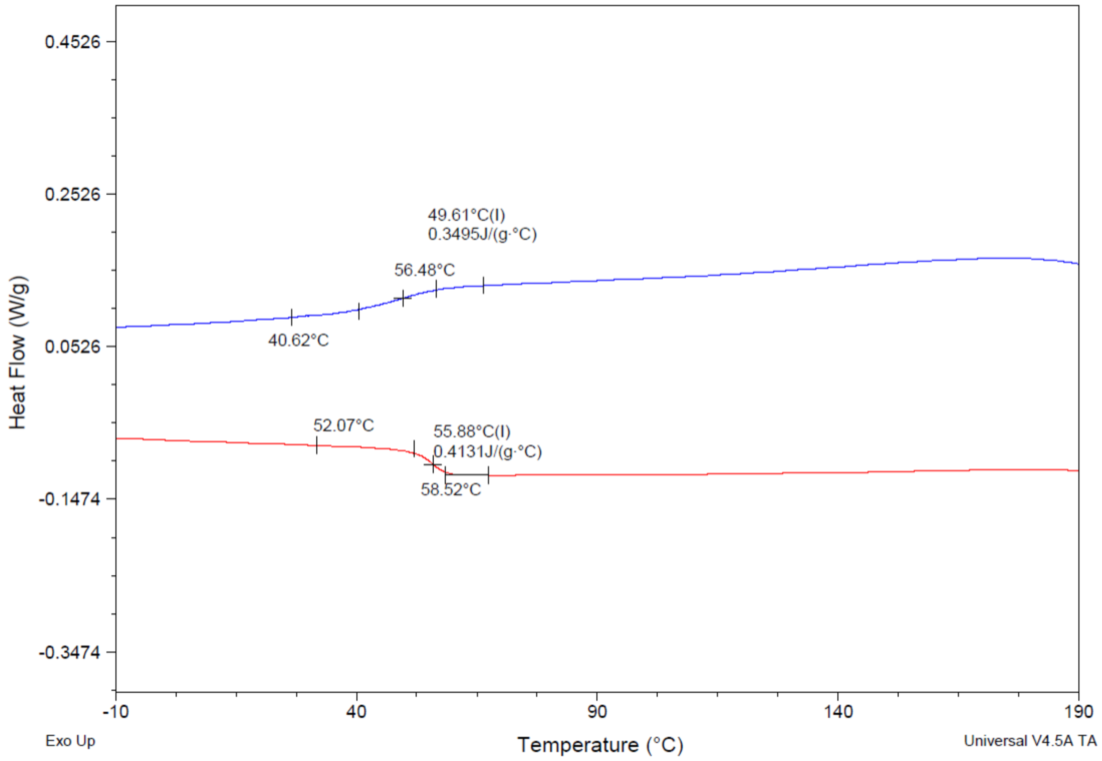

Heat-cool-heat-cool-heat over a -60 to 200 °C temperature range (10 °C/min), only final cool-heat cycle shown over the range -10 to 190 °C.

Figure S6g. Modulated differential scanning calorimetry analysis of P-**3-7**

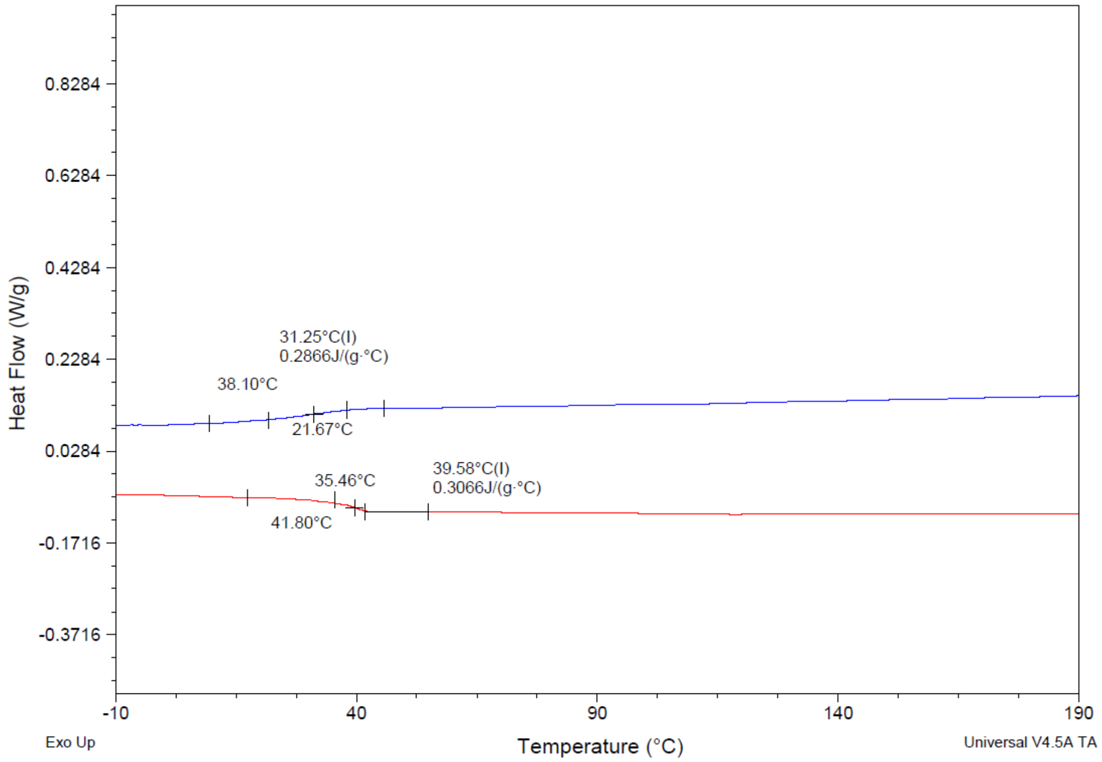

Heat-cool-heat-cool-heat over a -60 to 200 °C temperature range (10 °C/min), only final cool-heat cycle shown over the range -10 to 190 °C.

Figure S6h. Modulated differential scanning calorimetry analysis of P-**3**-**7**-24h

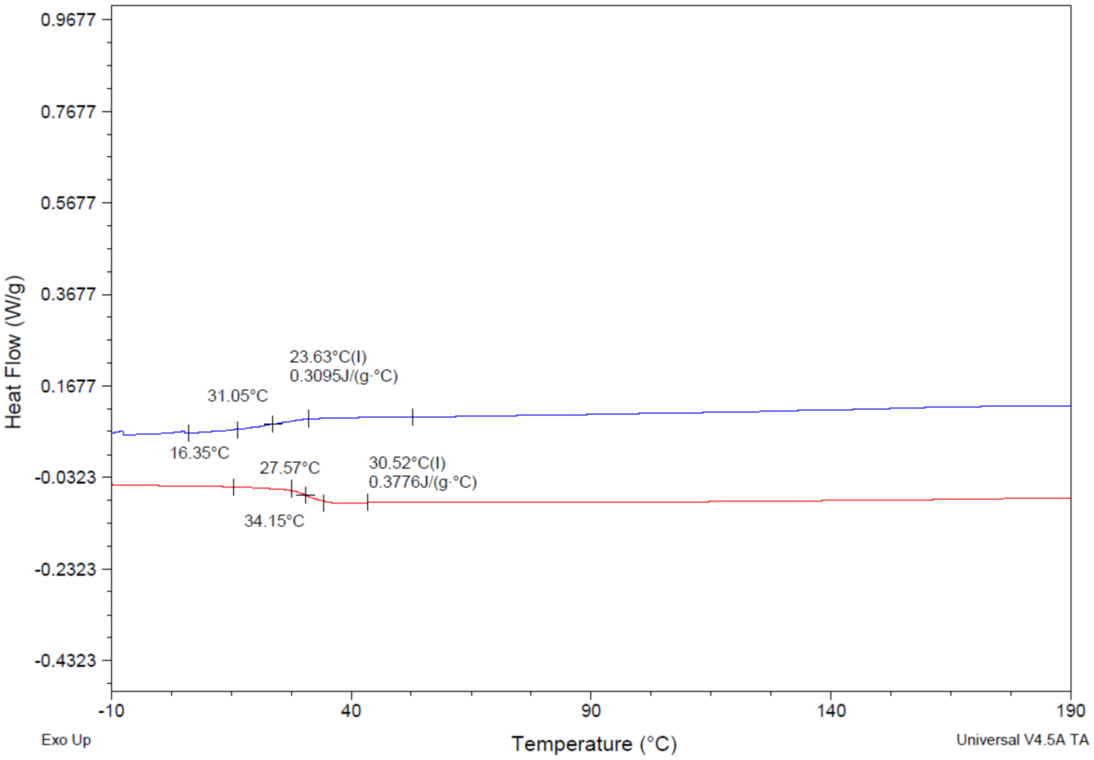

Heat-cool-heat-cool-heat over a -60 to 200 °C temperature range (10 °C/min), only final cool-heat cycle shown over the range -10 to 190 °C.

Figure S6i. Modulated differential scanning calorimetry analysis of P-**3**-**15**

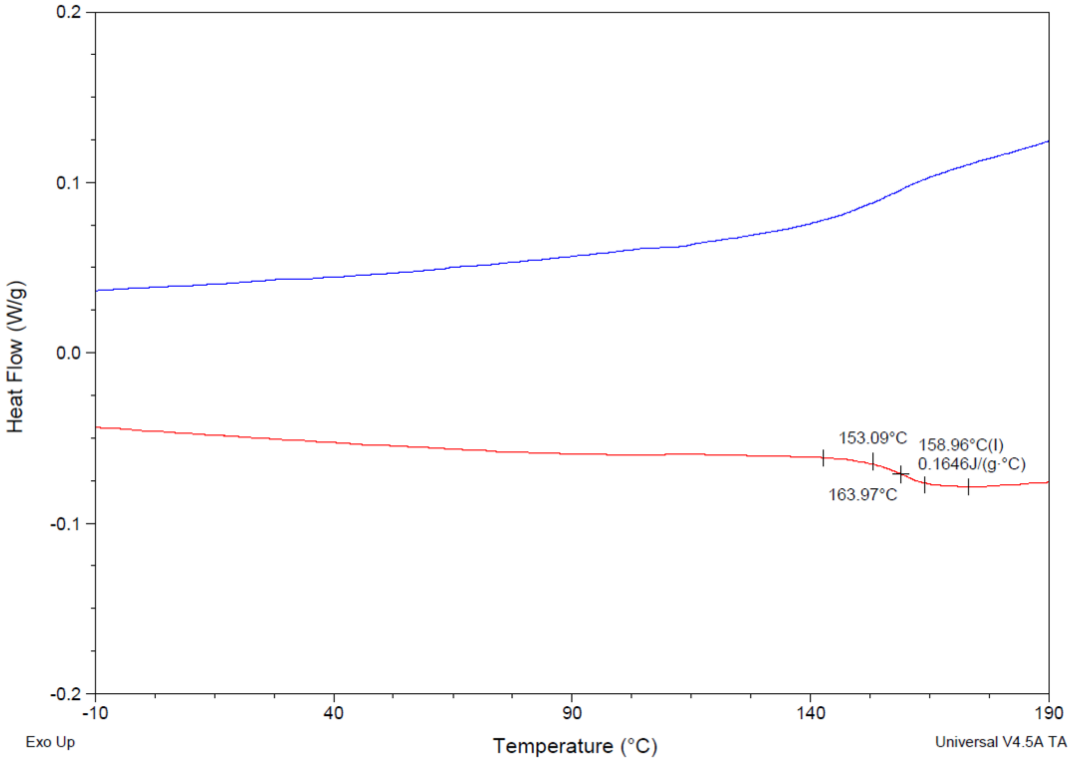

Heat-cool-heat-cool-heat over a -60 to 200 °C temperature range (10 °C/min), only final cool-heat cycle shown over the range -10 to 190 °C.

Figure S6j. Modulated differential scanning calorimetry analysis of CP-**13-15-14**

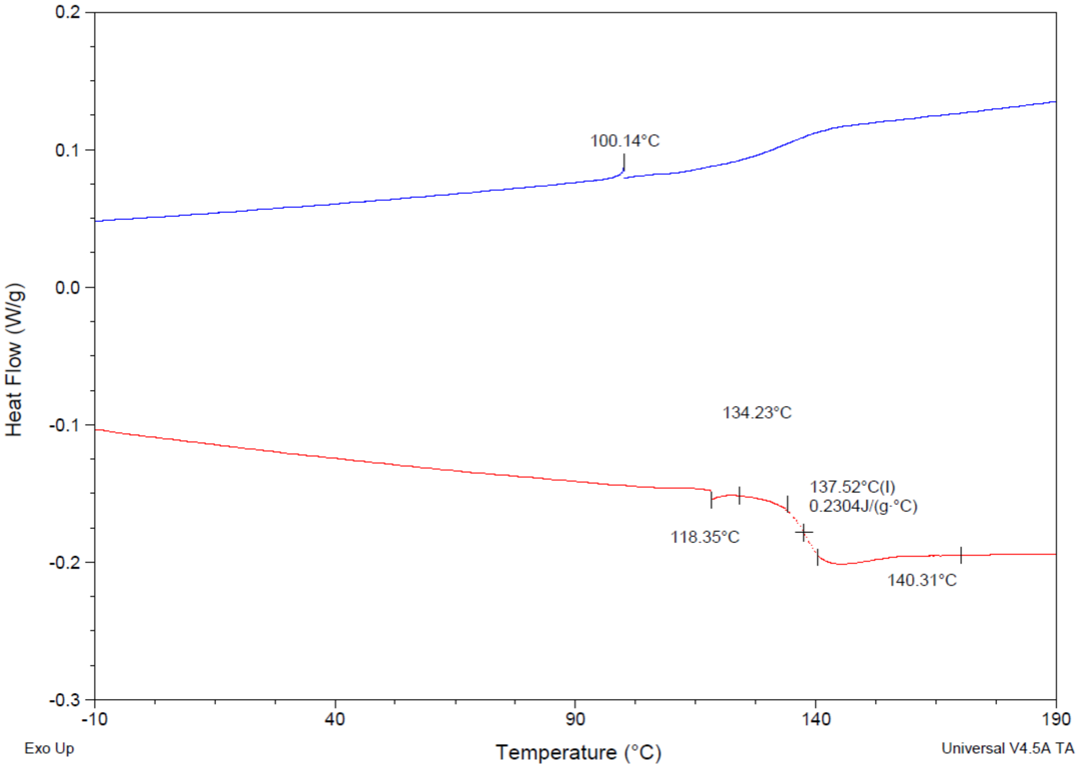

Heat-cool-heat-cool-heat over a -60 to 200 °C temperature range (10 °C/min), only final cool-heat cycle shown over the range -10 to 190 °C. Peak at 100.1 °C in the cool cycle is an artefact of the chiller unit and not related to the sample.

Figure S6k. Modulated differential scanning calorimetry analysis of CP-**13-15-10**

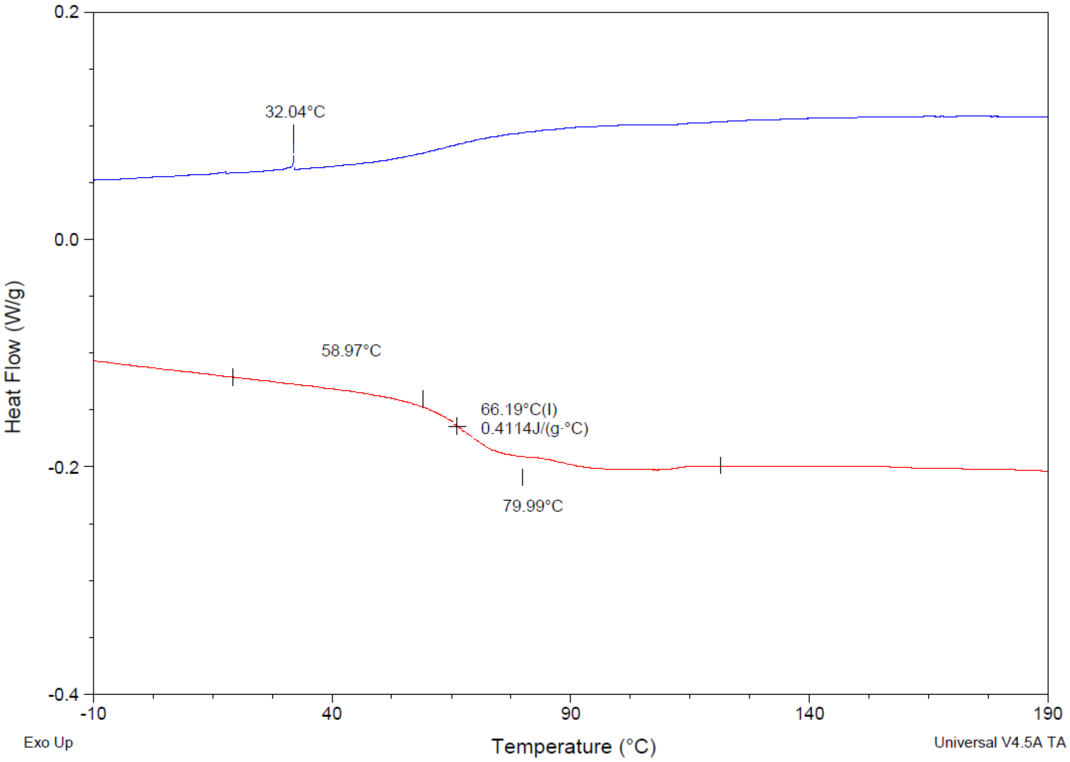

Heat-cool-heat-cool-heat over a -60 to 200 °C temperature range (10 °C/min), only final cool-heat cycle shown over the range -10 to 190 °C. Peak at 32.0 °C in the cool cycle is an artefact of the chiller unit and not related to the sample.

Figure S6l. Modulated differential scanning calorimetry analysis of CP-**13-15-7**

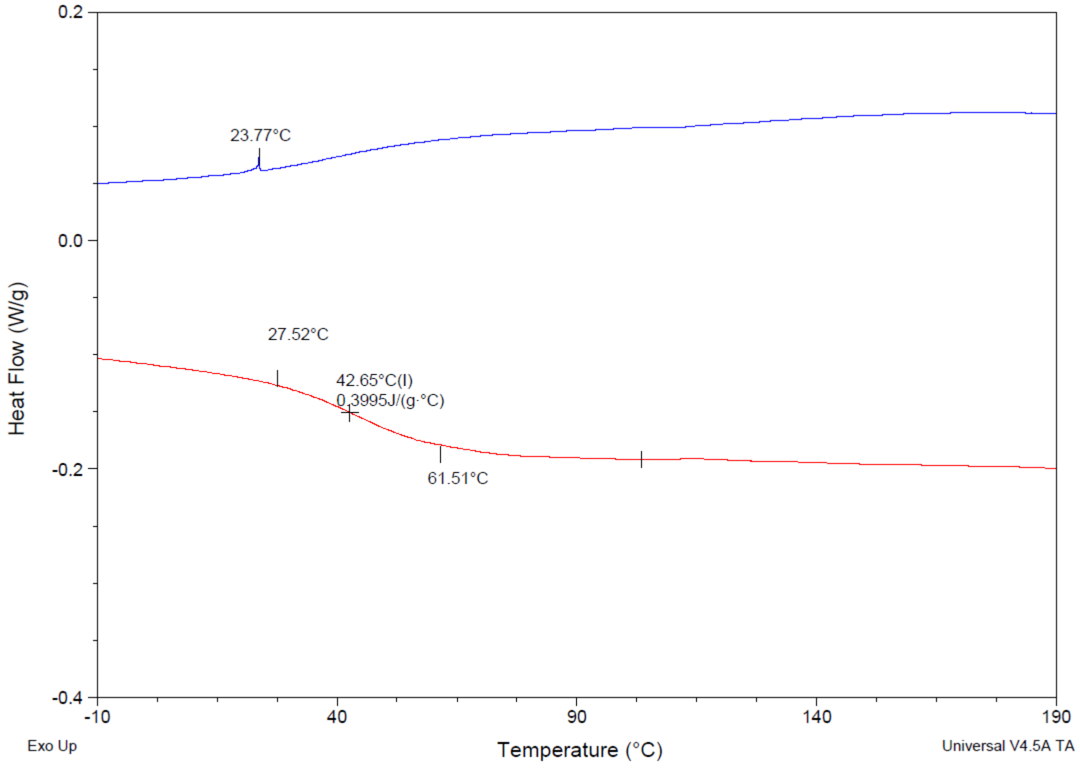

Heat-cool-heat-cool-heat over a -60 to 200 °C temperature range (10 °C/min), only final cool-heat cycle shown over the range -10 to 190 °C. Peak at 23.8 °C in the cool cycle is an artefact of the chiller unit and not related to the sample.

Figure S6m. Modulated differential scanning calorimetry analysis of CP-**3-15-14**

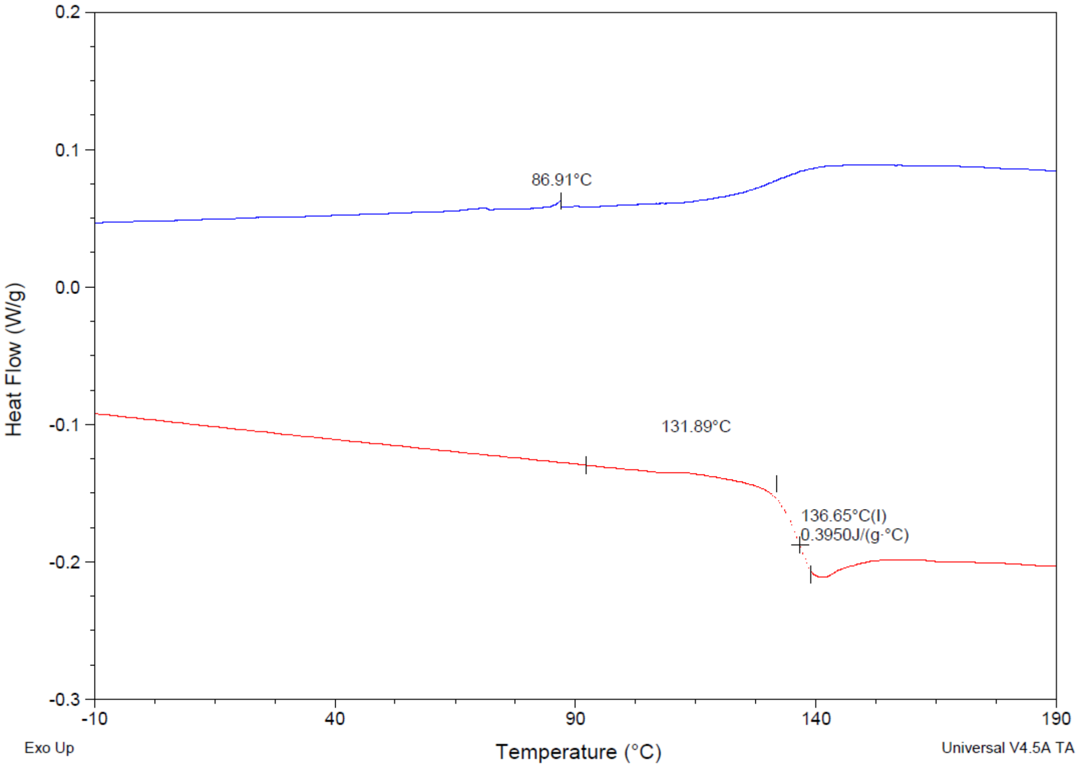

Heat-cool-heat-cool-heat over a -60 to 200 °C temperature range (10 °C/min), only final cool-heat cycle shown over the range -10 to 190 °C. Peak at 86.9 °C in the cool cycle is an artefact of the chiller unit and not related to the sample.

Figure S6n. Modulated differential scanning calorimetry analysis of CP-**3-15-10**

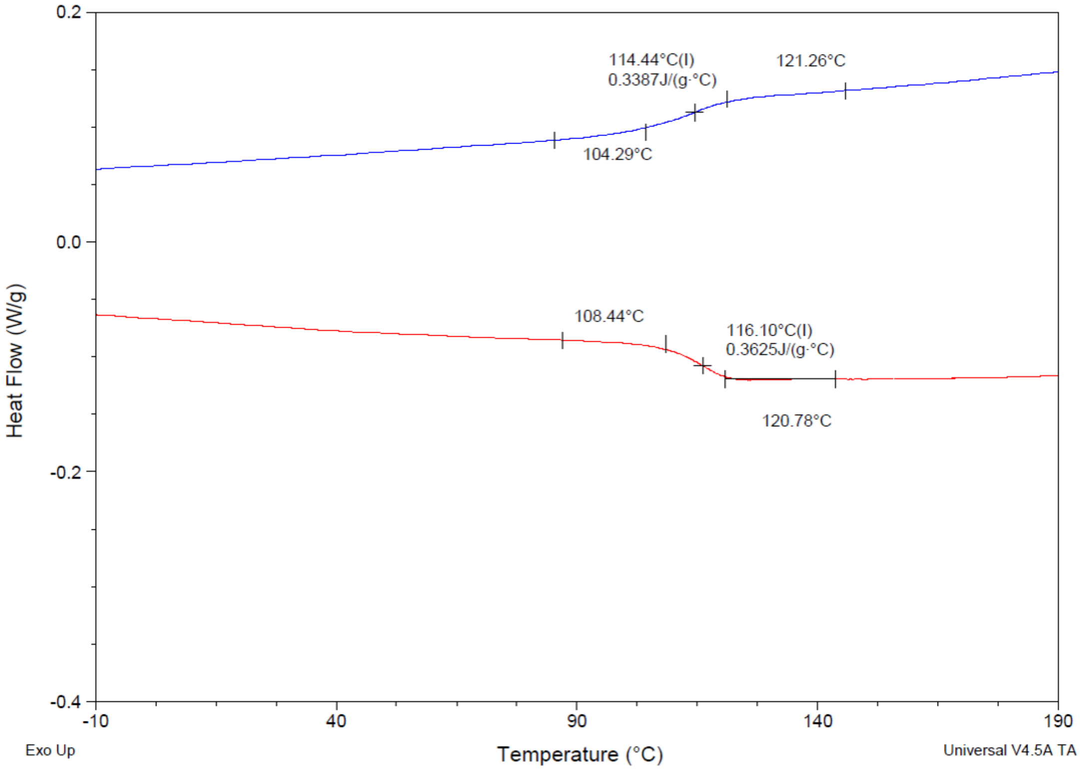

Heat-cool-heat-cool-heat over a -60 to 200 °C temperature range (10 °C/min), only final cool-heat cycle shown over the range -10 to 190 °C.

Figure S6o. Modulated differential scanning calorimetry analysis of CP-**3-15-7**

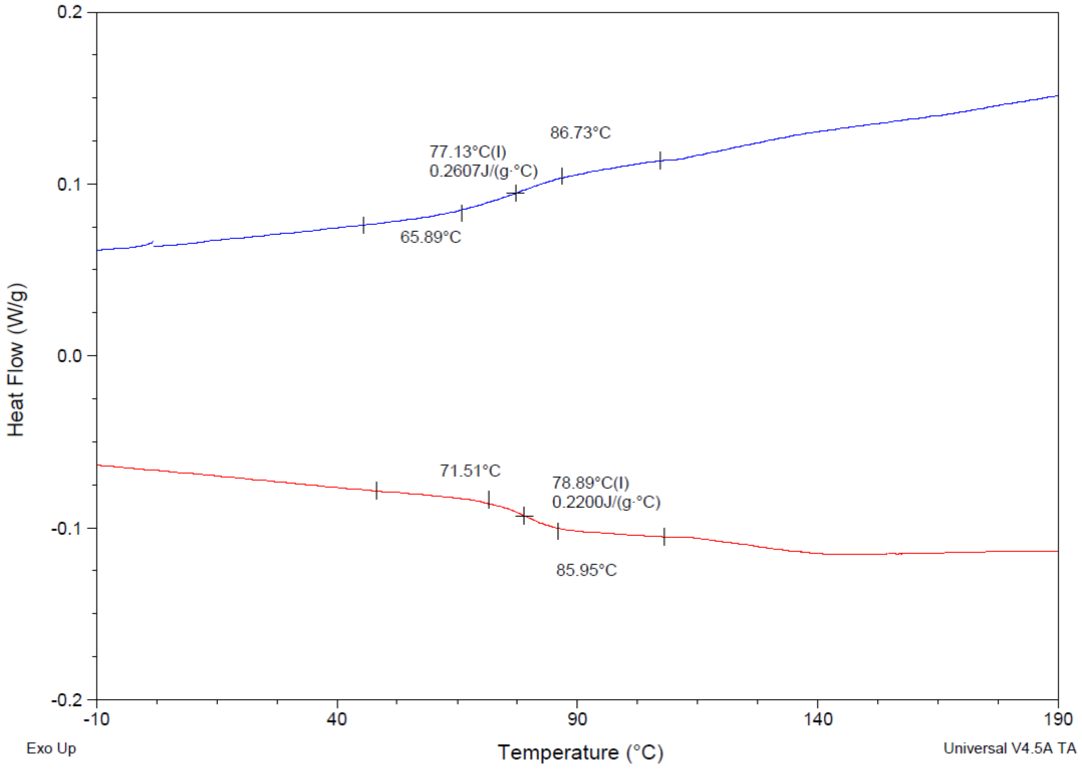

Heat-cool-heat-cool-heat over a -60 to 200 °C temperature range (10 °C/min), only final cool-heat cycle shown over the range -10 to 190 °C.

Figure S6p. Modulated differential scanning calorimetry analysis of CP-**3-15-7**-25%iso

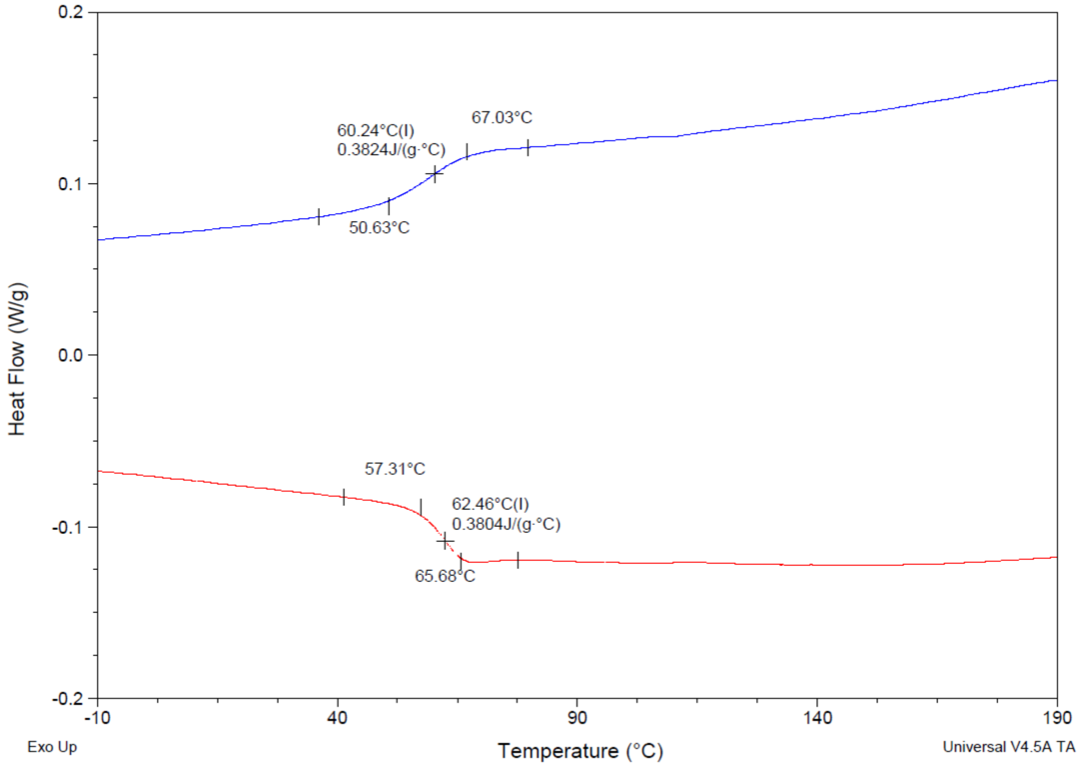

Heat-cool-heat-cool-heat over a -60 to 200 °C temperature range (10 °C/min), only final cool-heat cycle shown over the range -10 to 190 °C.

Figure S6q. Modulated differential scanning calorimetry analysis of TP-**4a-14**

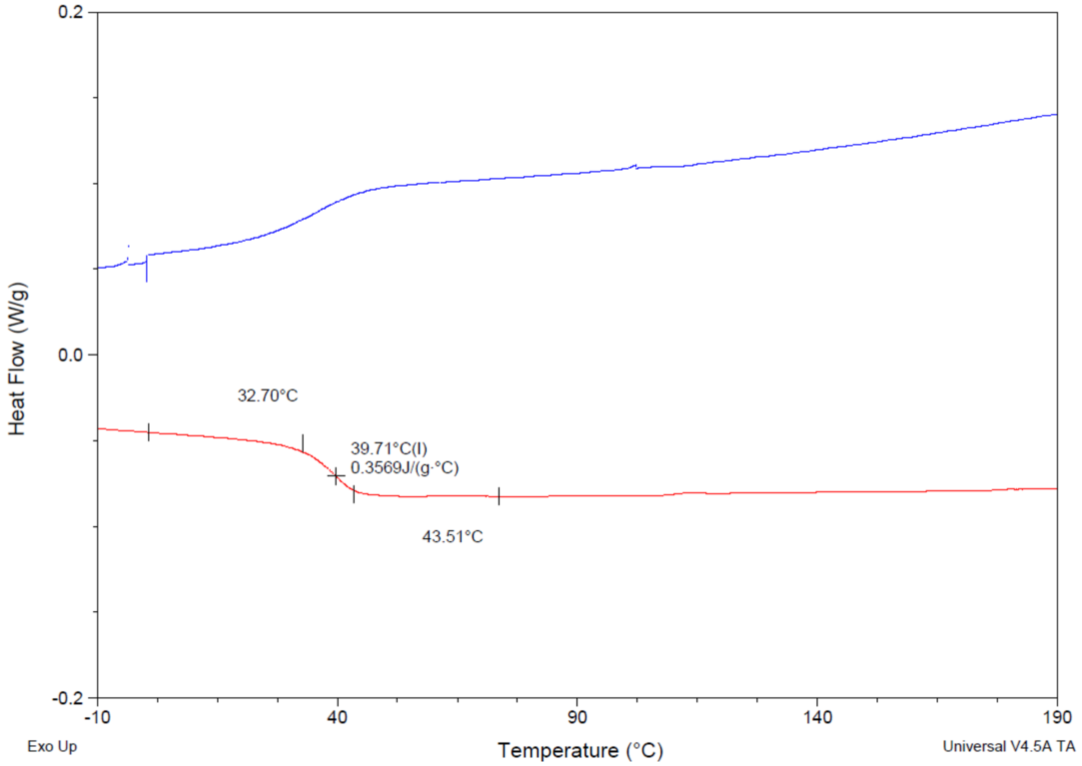

Heat-cool-heat-cool-heat over a -60 to 200 °C temperature range (10 °C/min), only final cool-heat cycle shown over the range -10 to 190 °C. Peaks at 0 to -5 °C in the cool cycle are an artefact of the chiller unit and not related to the sample.

Figure S6r. Modulated differential scanning calorimetry analysis of TP-**4a-10**

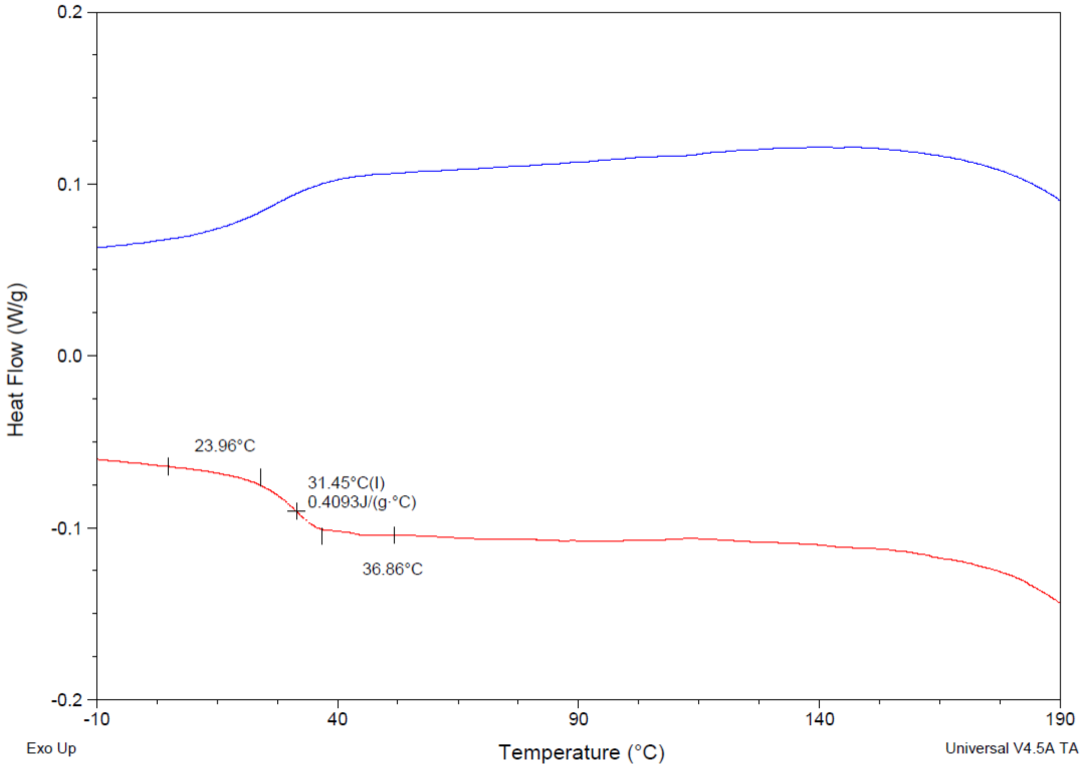

Heat-cool-heat-cool-heat over a -60 to 200 °C temperature range (10 °C/min), only final cool-heat cycle shown over the range -10 to 190 °C.

Figure S6s. Modulated differential scanning calorimetry analysis of TP-**4a-7**

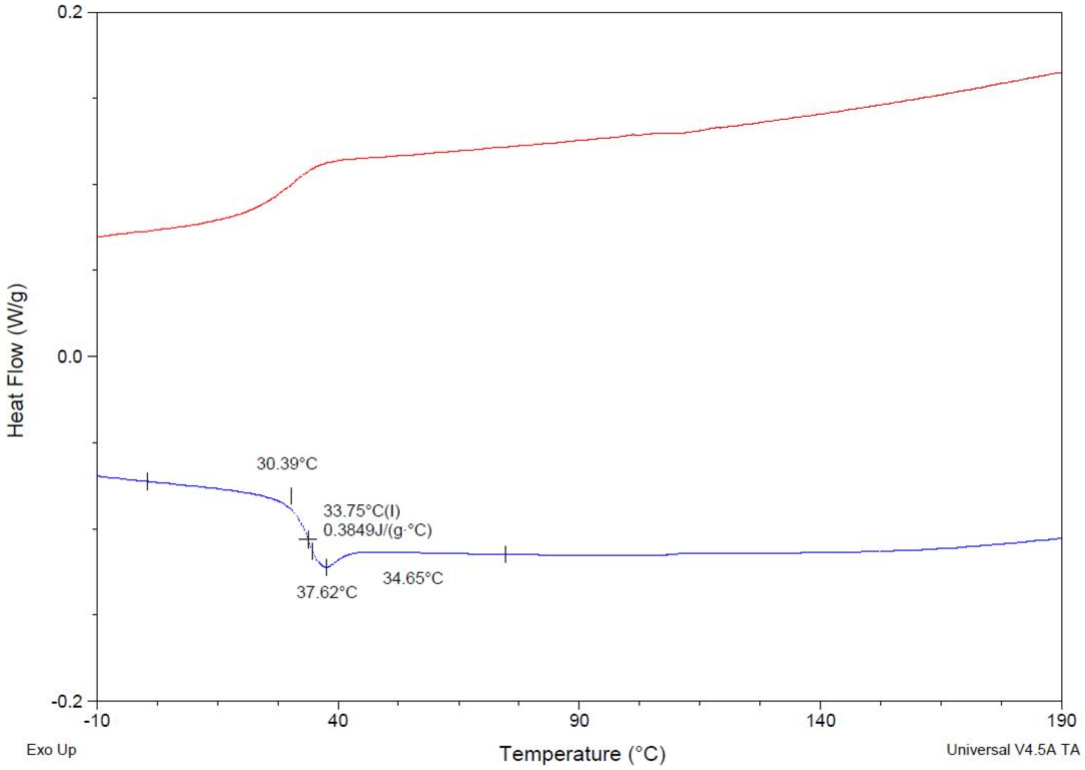

Heat-cool-heat-cool-heat over a -60 to 200 °C temperature range (10 °C/min), only final cool-heat cycle shown over the range -10 to 190 °C.

Figure S6t. Modulated differential scanning calorimetry analysis of TP-**17-14**

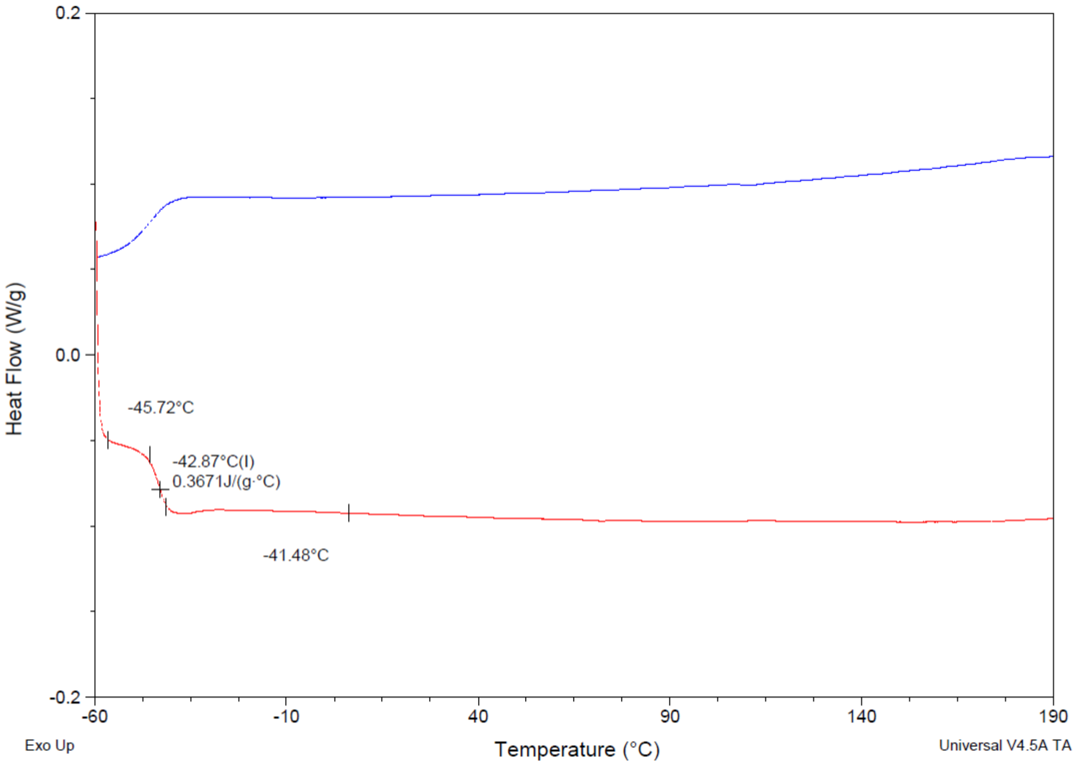

Heat-cool-heat-cool-heat over a -60 to 200 °C temperature range (10 °C/min), only final cool-heat cycle shown over the range -60 to 190 °C.

Figure S6u. Modulated differential scanning calorimetry analysis of TP-**17-10**

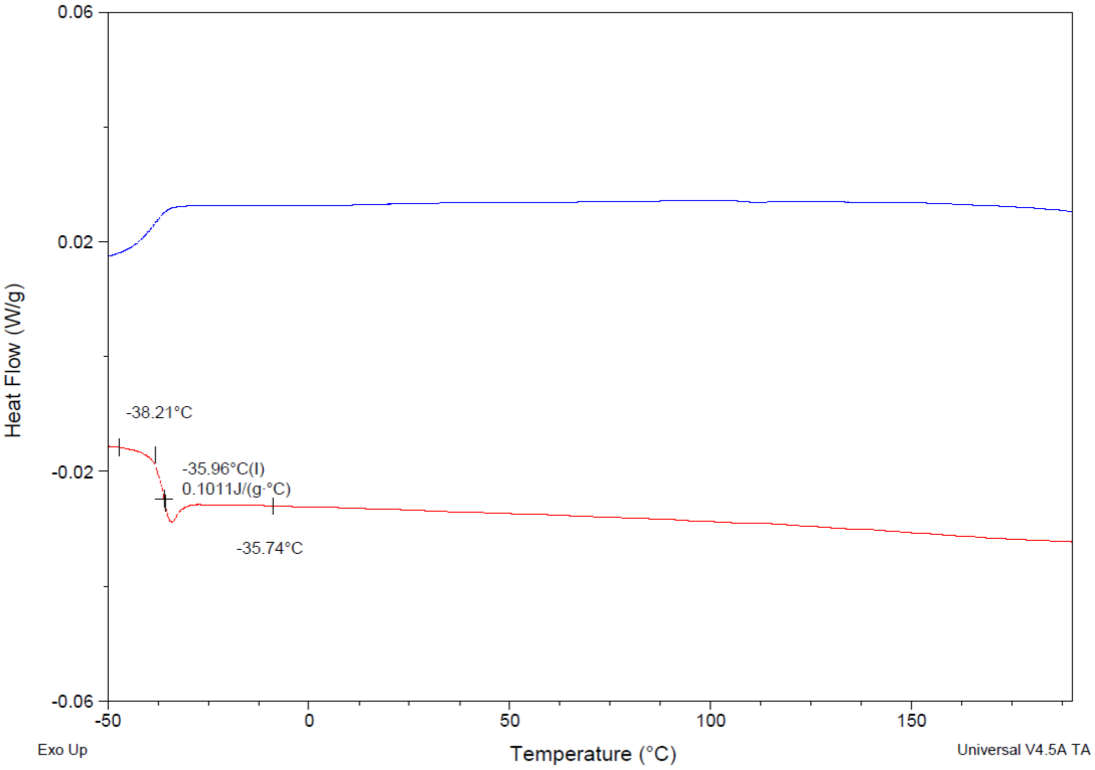

Heat-cool-heat-cool-heat over a -60 to 200 °C temperature range (10 °C/min), only final cool-heat cycle shown over the range -50 to 190 °C.

Figure S6v. Modulated differential scanning calorimetry analysis of TP-**17-7**

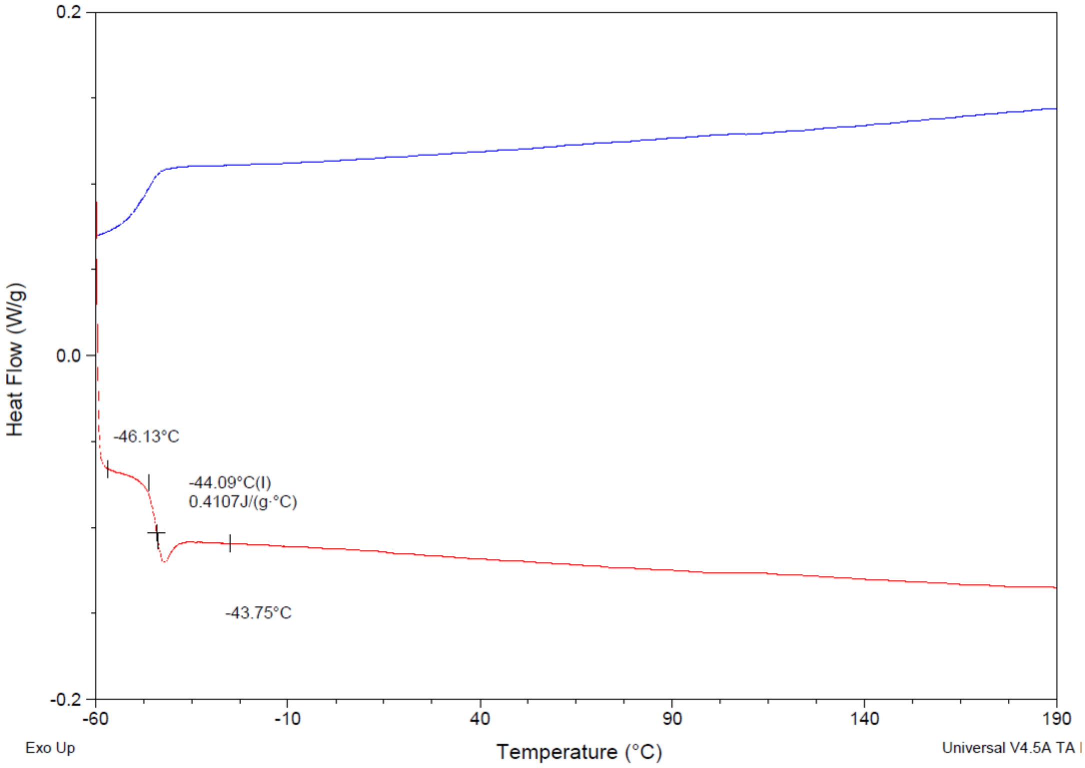

Heat-cool-heat-cool-heat over a -60 to 200 °C temperature range (10 °C/min), only final cool-heat cycle shown over the range -60 to 190 °C.

Figure S6w. Modulated differential scanning calorimetry analysis of TCP-**4a-17-10**

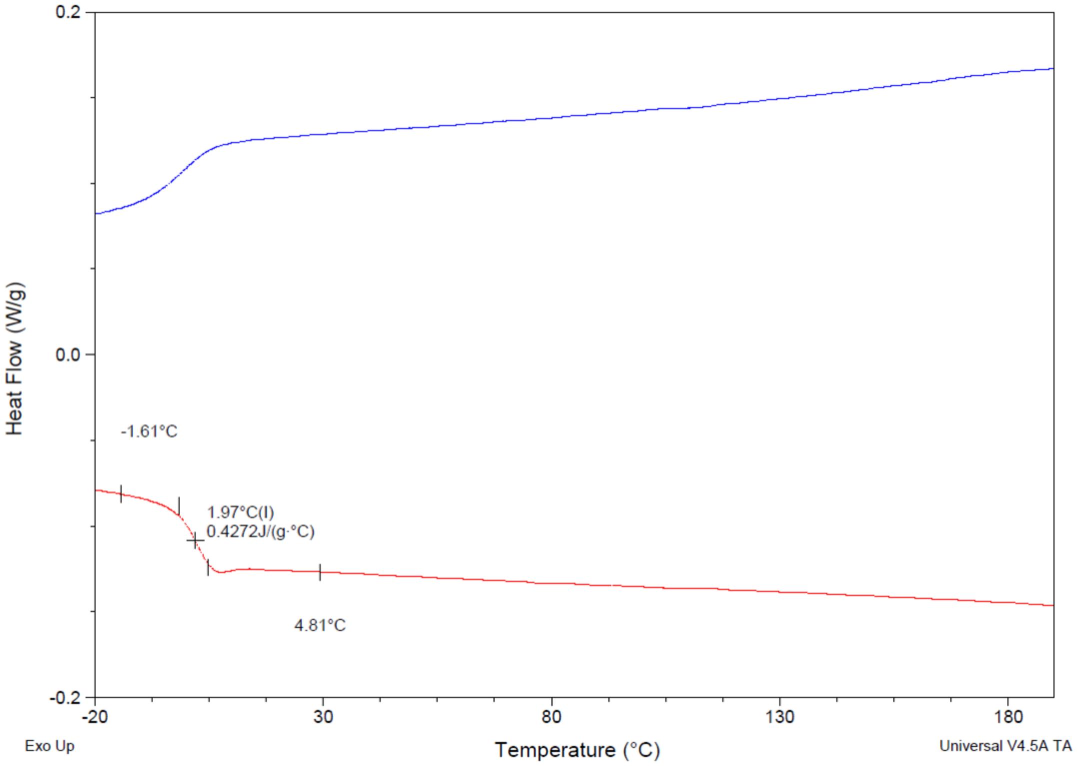

Heat-cool-heat-cool-heat over a -60 to 200 °C temperature range (10 °C/min), only final cool-heat cycle shown over the range -20 to 190 °C.

Figure S6x. Modulated differential scanning calorimetry analysis of TCP-**4a-17-7**

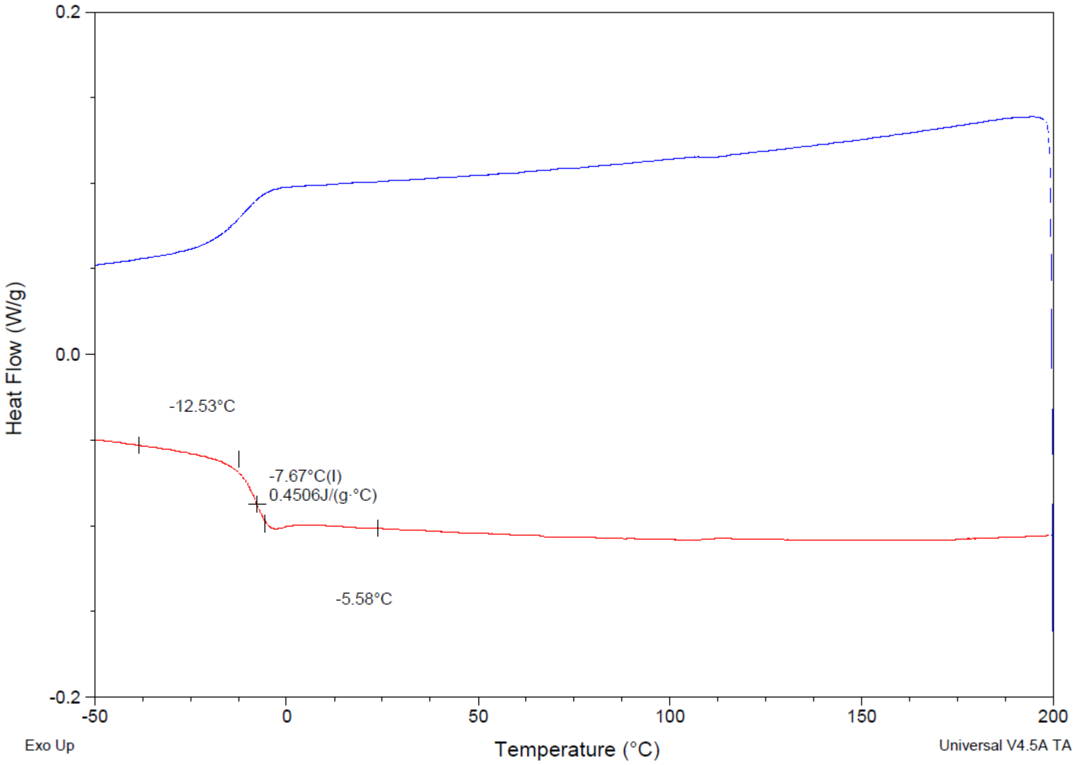

Heat-cool-heat-cool-heat over a -60 to 200 °C temperature range (10 °C/min), only final cool-heat cycle shown over the range -500 to 190 °C.

Description of physical appearance of polymers

Table S2. Description of physical appearance of polymers

Polymer	**Appearance**
P-**13**-**14**	white brittle solid/powder
P-**13**-**10**	white brittle solid/powder
P-**13**-**7**	light brown brittle solid
P-**13**-**15**	white powder
P-**3**-**14**	very light yellow brittle solid
P-**3**-**10**	light brown brittle solid
P-**3**-**7**	light brown brittle solid
P-**3**-**7**-24h	yellow brittle solid
P-**3**-**15**	white powder
CP-**13**-**15**-**14**	white powder
CP-**13**-**15**-**10**	white brittle solid
CP-**13**-**15**-**7**	white powder
CP-**3**-**15**-**14**	very light brown brittle solid
CP-**3**-**15**-**10**	very light brown brittle solid
CP-**3**-**15**-**7**	very light brown brittle solid
CP-**3**-**15**-**7**-25%iso	light brown brittle solid
TP-**4a**-**14**	brown glassy solid, brittle
TP-**4a**-**10**	light brown glassy solid, brittle
TP-**4a**-**7**	golden glassy solid, brittle
TP-**17**-**14**	red, sticky gum
TP-**17**-**10**	golden, sticky gum
TP-**17**-**7**	golden, tacky gum
TCP-**4a**-**17**-**10**	golden, tough, flexible solid
TCP-**4a**-**17**-**7**	light brown, deformable solid

Description of naming of polymer samples

Prefix “P” for polymers made using the diacid chloride procedure of a reaction between one diacid chloride and one diol. First number refers to diacid chloride and corresponds to the numbering of structures in the paper. Second number refers to diol used and corresponds to the numbering of structures in the paper.

Prefix “CP” for co-polymers made using the diacid chloride procedure of a reaction between one diacid chloride and two diols. First number refers to diacid chloride and corresponds to the numbering of structures in the paper. Second and third number refers to the two different diols used and corresponds to the numbering of structures in the paper.

Prefix “TP” for polymers made using the diester tranesterification procedure of a reaction between one diester and one diol. First number refers to the diester and corresponds to the numbering of structures in the paper. Second number refers to diol used and corresponds to the numbering of structures in the paper.

Prefix “TCP” for co-polymers made using the diester tranesterification procedure of a reaction between two diesters and one diol. First and second numbers refer to the two different diesters and corresponds to the numbering of structures in the paper. Third number refers to diol used and corresponds to the numbering of structures in the paper.

Synthesis of branched monomers 20, 22 and 23

Dimethyl 3-ethyl-4-methylpimelate 20. A solution of the angelica lactone dimer **19** (674 mg, 3.44 mmol), 10% Pd/C (35 mg, 5 wt%) and La(OTf)$_3$ (51 mg, 7.5 wt%) in methanol (6 mL) was introduced to a Parr pressure vessel. The reactor was sealed, flushed with hydrogen three times and finally pressurized to 20 bar. The mixture was stirred at rt for 30 min before being heated to 220 °C. The reaction was kept at 220 °C for 10 h and then quickly cooled in an ice-water bath. The pressure was gently released and the vessel was opened and thoroughly rinsed with acetone. The contents of the reactor were transferred into a 250 mL volumetric flask and tetradecane (271 mg) was added as an internal standard. The mixture was diluted to the exact volume by further addition of acetone for analysis by GC-MS, which indicated a yield of 62%. The solvent was evaporated and the product purified by silica gel column chromatography (ethyl acetate/hexanes= 1/7 to 1/5) to give dimethyl 3-ethyl-4-methylpimelate **20** as a colorless liquid (474 mg, 60%). ^{1}H NMR (CDCl$_3$, 600 MHz): δ 3.61 (m, 6H), 2.4-2.2 (m, 4H), 1.79-1.08 (m, 6H), 0.86-0.73 (m, 6H). ^{13}C NMR (CDCl$_3$, 150 MHz): δ 174.3, 174.2, 174.1, 51.4, 51.4, 51.4, 41.2, 40.7, 35.9, 34.9, 34.4, 33.8, 32.3, 32.2, 29.1, 28.4, 24.4, 22.6, 15.3, 14.7, 11.9, 11.7. M.S. (EI): *m/z* (% of max intensity) 59(43), 69(27), 73(39), 74(47), 81(17), 83(92), 87(17), 97(60), 115(51), 124(15), 125(84), 157(85), 167(16), 199(16).

GC-MS Yield Calculation for 20. Dimethyl 3-ethyl-4-methylpimelate **20** (98 mg) and tetradecane (61 mg) were added into a 50 mL volumetric flask and diluted with acetone to the exact volume. GC-MS analysis was calibrated using this stock solution prior to the injection of the reaction sample.

Calibration 1: Area of tetradecane 39352948, area of dimethyl 3-ethyl-4-methylheptanedioate 50569001;

Calibration 2: Area of tetradecane 38118201, area of dimethyl 3-ethyl-4-methylheptanedioate 48573468;

Response factor (R)=

$$\frac{area\ of\ diester}{mass\ of\ diester}\times\frac{mass\ of\ C14}{area\ of\ C14}$$

R$_{avg}$ = (R$_1$+R$_2$)/2 = (0.7999+0.7932)/2 = 0.7966

Amount of dimethyl 3-ethyl-4-methylheptanedioate in the 250 mL volumetric flask =

$$\frac{area\ of\ diester}{R}\times\frac{mass\ of\ C14}{area\ of\ C14}=\frac{48500081}{0.7966}\times\frac{0.271g}{33916072}=0.487\ g$$

Theoretical yield of dimethyl 3-ethyl-4-methylheptanedioate from 0.674 g ALD =

$$\frac{0.674\ g}{196\ g/mol}\times\ 230\ g/mol=0.791\ g$$

Molar yield of dimethyl 3-ethyl-4-methylheptanedioate by GC-MS =

$$\frac{0.487\ g}{0.791\ g}\times 100=62\%$$

Figure S7. GC-MS chromatogram of the liquid products obtained after the ring-opening reaction of angelica lactone dimer.

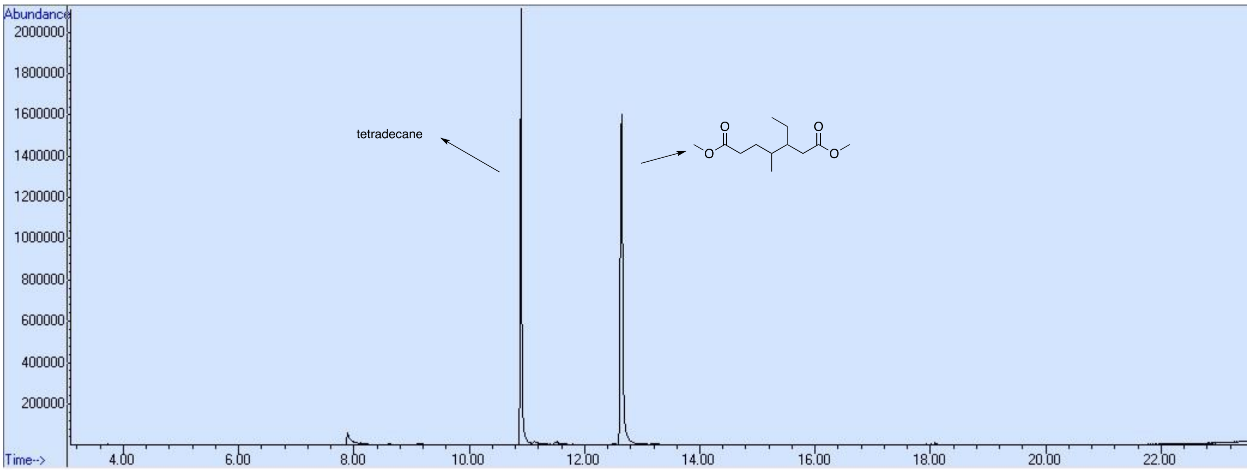

Ethyl 3-(carbethoxymethyl)-2,4-dimethylcyclopenta-1,3-diene-1-carboxylate 22. Sodium metal (8.0 g, 348 mmol) was dissolved in absolute ethanol (200 mL) and the volume of the solution was reduced to *ca.* 100 mL under vacuum. The resulting viscous mixture was added dropwise with good stirring to a mixture of ethyl levulinate (50.0 g, 347 mmol), powdered CaO (30 g), and absolute ethanol (50 mL) cooled in an ice-salt bath. The ice was allowed to melt and the reaction was left to stir for 70 h, during which time the color changed from yellow to red and from free flowing to a gel-like consistency. The reaction mixture was filtered and the solids were washed with ethanol. Ethanolic HCl was added to the filtrate until the pH was 2-3. The volatiles were evaporated resulting in a viscous, dark yellow oil (20.0 g), which was dissolved in absolute ethanol (100 mL). Concentrated sulfuric acid (10 drops) was added and the mixture was heated at reflux for 24 h. Most of the ethanol was evaporated and the residue was diluted with water and extracted with dichloromethane. Removal of the solvent gave the crude product, a sample of which (4.22 g) was purified by silica gel chromatography (dichloromethane) to give **22** as a yellow oil (1.80 g). ^{1}H NMR (400 MHz, $CDCl_3$) δ 4.22 (q, *J* = 7.1 Hz, 2H), 4.15 (q, *J* = 7.1 Hz, 2H), 3.34-3.29 (m, 2H), 3.24 (q, *J* = 2.4 Hz, 2H), 2.32 (t, *J* = 2.4 Hz, 3H), 2.05 (s, 3H), 1.31 (t, *J* = 7.1 Hz, 3H), 1.26 (t, *J* = 7.1 Hz, 3H). ^{13}C NMR (100 MHz, $CDCl_3$) δ 170.9, 165.0, 156.1, 146.7, 134.7, 126.5, 60.8, 59.3, 45.4, 31.4, 14.5, 14.2, 14.2, 13.6.

Ethyl 3-(carbethoxymethyl)-2,4-dimethylcyclopentane-1-carboxylate 23. A solution of diene **22** (0.91 g, 3.6 mmol) in ethanol (20 mL) was introduced into a Parr reactor. 10% Pd/C (180 mg) was added and the vessel was sealed, flushed with H_2, and pressurized to 12 bar. The reaction was heated at 80 °C for 6 h with vigorous stirring. The reactor was cooled and the reaction mixture was filtered. Evaporation of the solvent gave **23** as a colorless oil (0.85 g, 92%). ^{13}C NMR (100 MHz, $CDCl_3$) δ 176.1, 176.1, 175.0, 174.6, 173.8, 173.4, 173.2, 173.0, 60.3, 60.2, 60.1, 60.0, 51.4, 51.1, 50.2, 50.0, 47.5, 46.9, 46.5, 46.2, 46.0, 45.1, 43.4, 42.4, 42.2, 42.0, 40.0, 39.9, 39.7, 39.3, 37.8, 37.5, 37.3, 36.7, 36.5, 35.9, 35.5, 34.7, 34.6, 34.6, 34.5, 34.3, 31.3, 19.4, 18.7, 18.4, 18.3, 17.9, 16.2, 16.0, 15.6, 15.3, 14.3, 14.3, 14.2, 14.2, 14.2, 11.8.

Spectroscopic data for branched monomers 20, 22 and 23

Figure S8. ^{1}H-NMR spectrum of dimethyl 3-ethyl-4-methylpimelate **20** in $CDCl_3$.

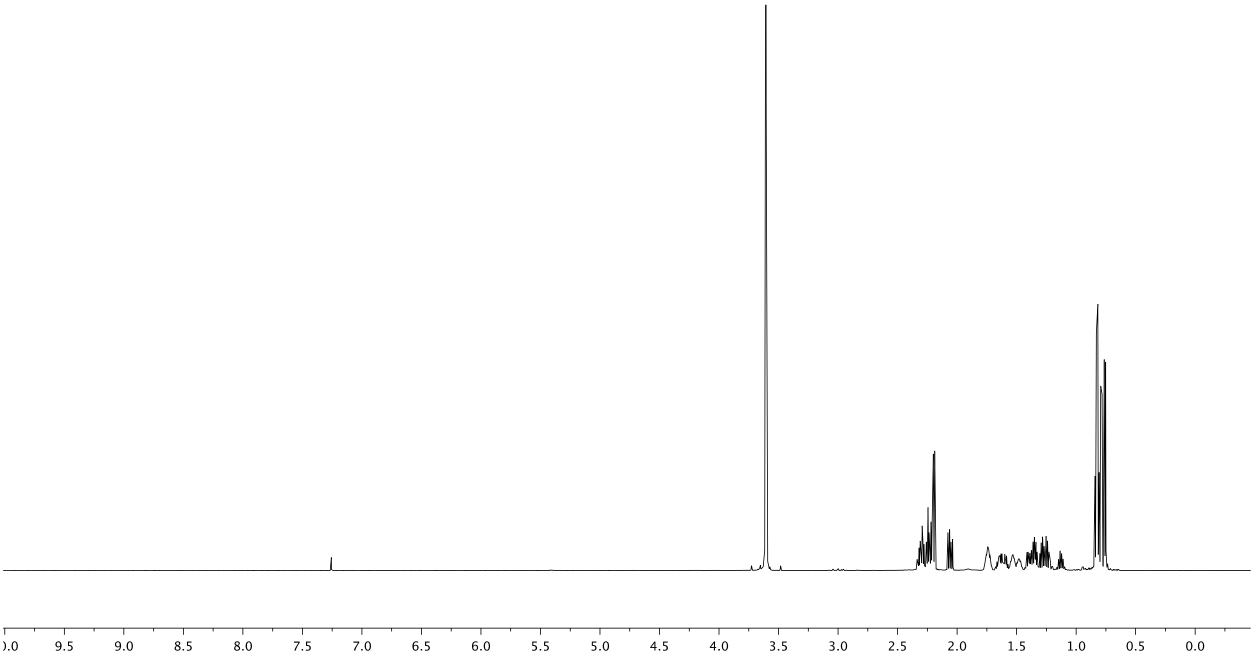

Figure S9. ^{13}C-NMR spectrum of dimethyl 3-ethyl-4-methylpimelate **20** in $CDCl_3$.

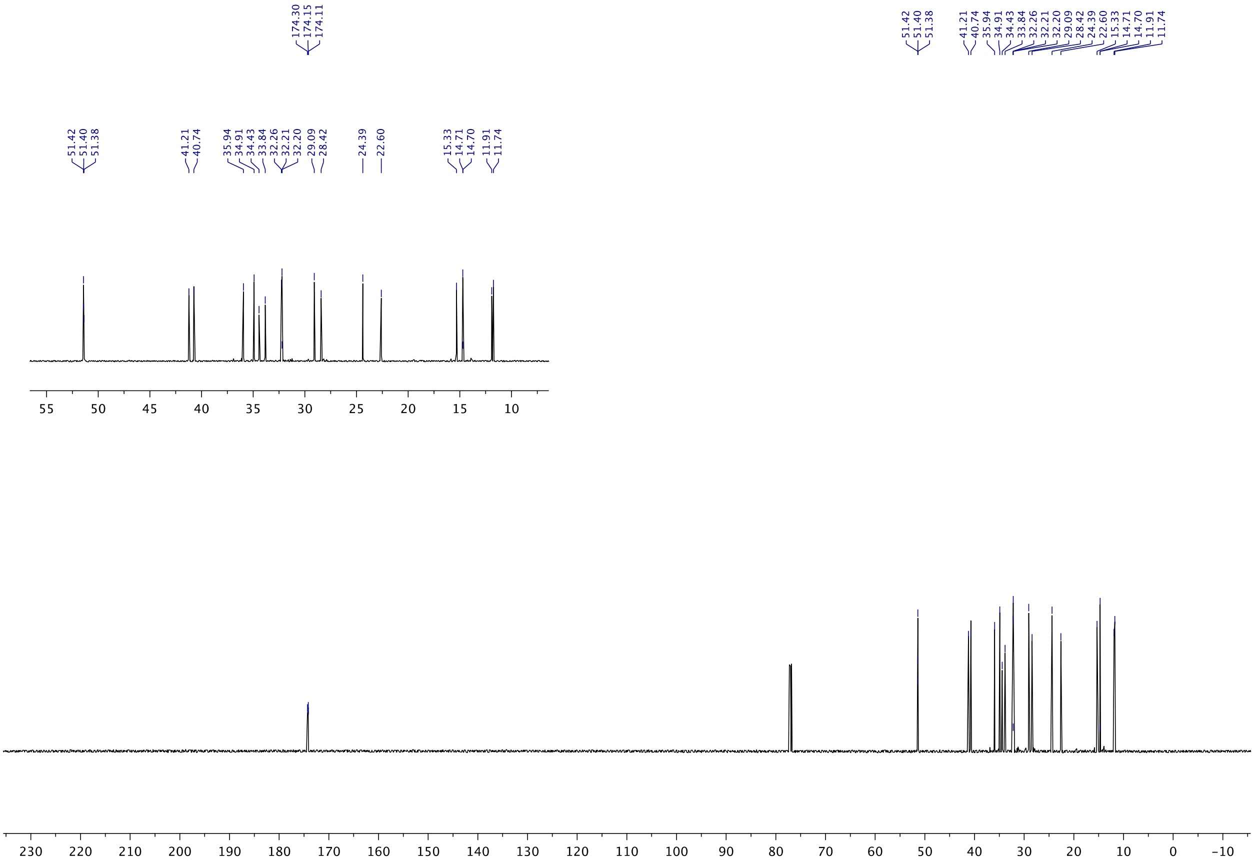

Figure S10. ^{1}H-NMR spectrum of ethyl 3-(carbethoxymethyl)-2,4-dimethylcyclopenta-1,3-diene-1-carboxylate **22** in $CDCl_3$.

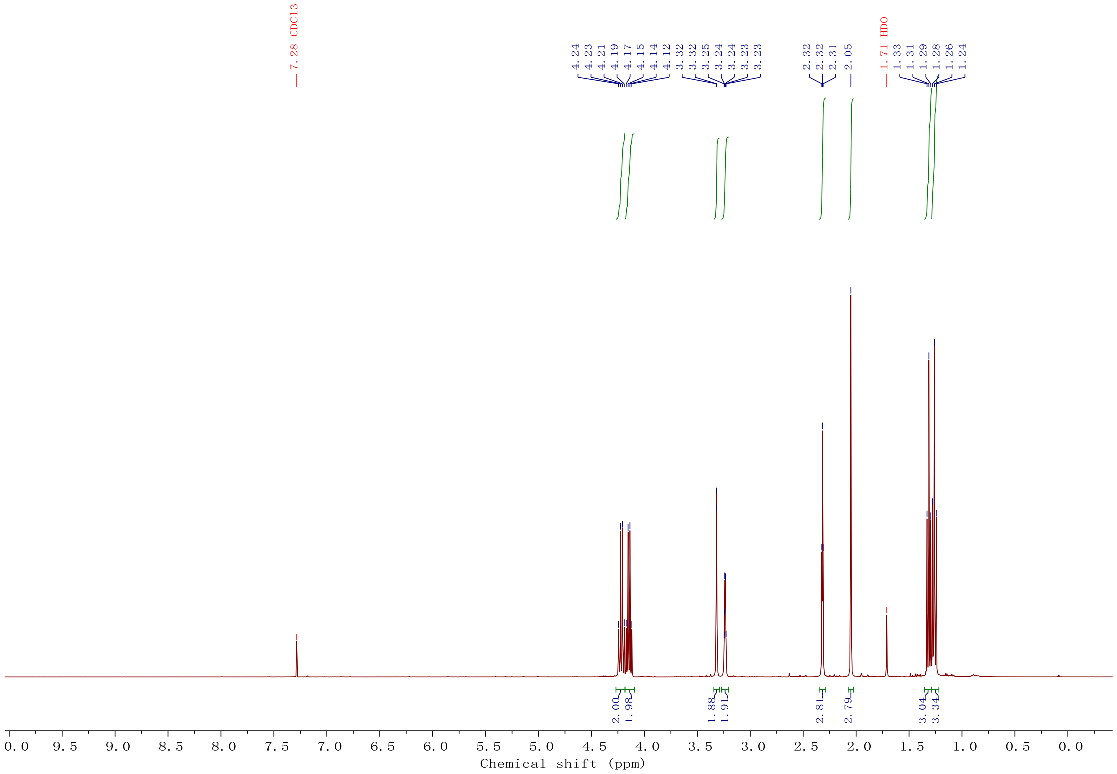

Figure S11. ^{13}C-NMR spectrum of ethyl 3-(carbethoxymethyl)-2,4-dimethylcyclopenta-1,3-diene-1-carboxylate **22** in $CDCl_3$.

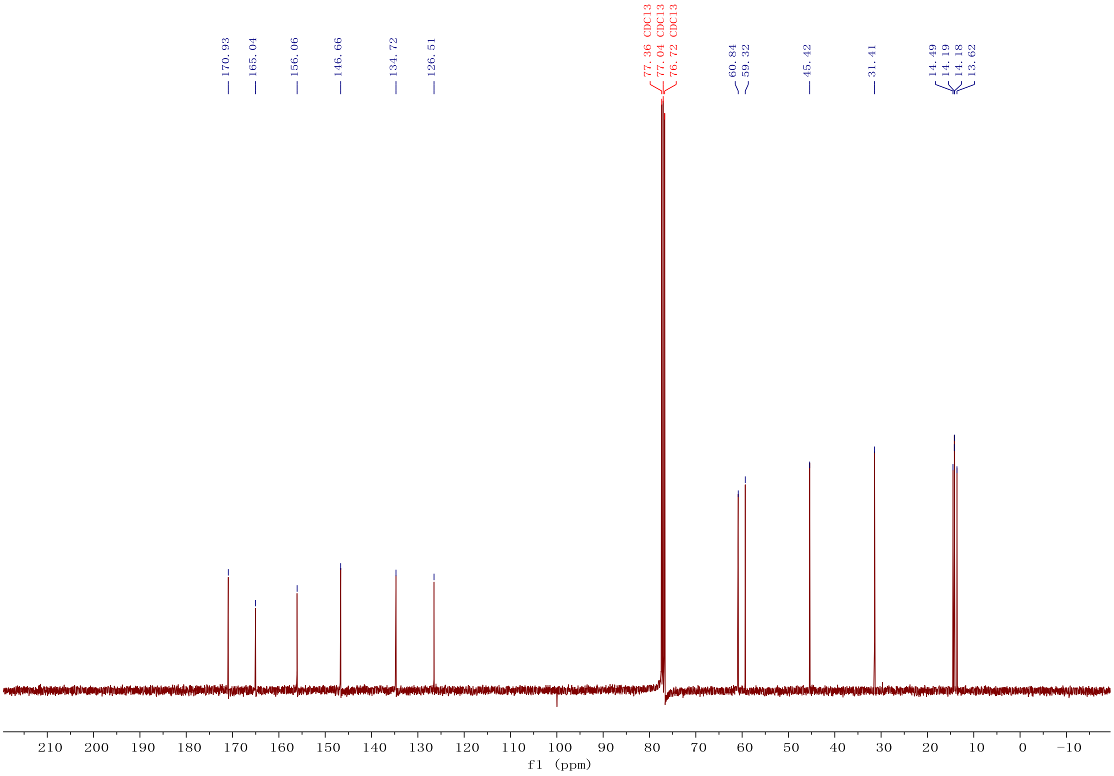

Figure S12. ^{1}H-NMR spectrum of ethyl 3-(carbethoxymethyl)-2,4-dimethylcyclopentane-1-carboxylate **23** in CDCl$_3$.

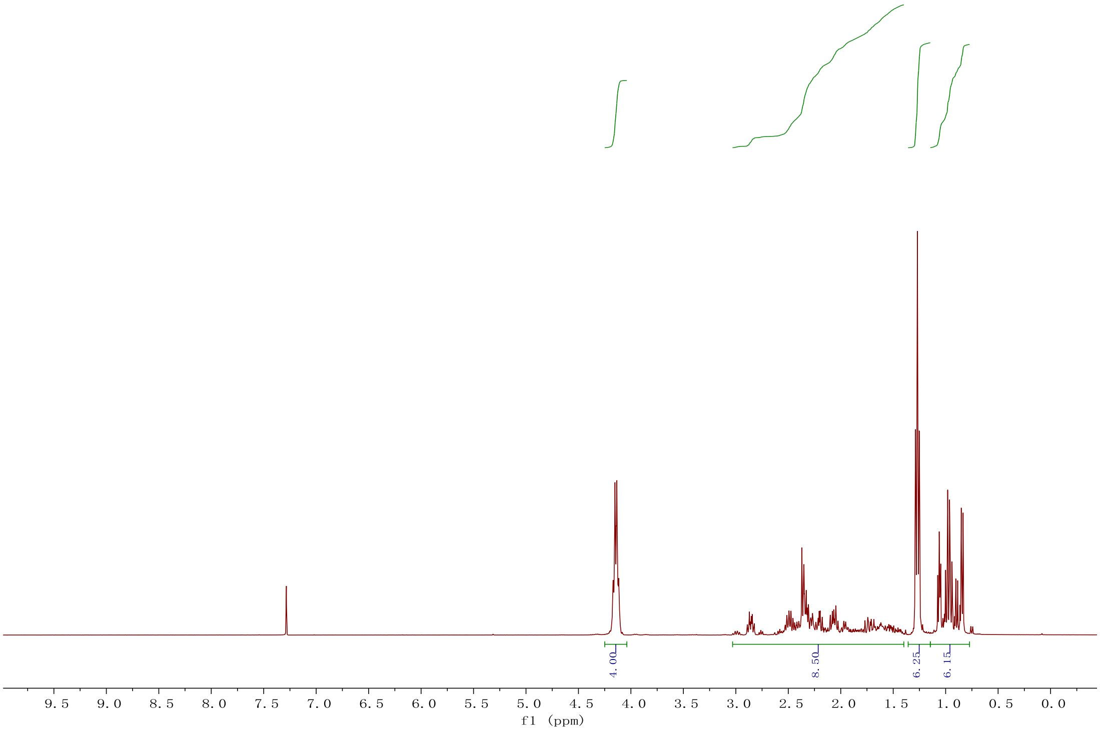

Figure S13. ^{13}C-NMR spectrum of ethyl 3-(carbethoxymethyl)-2,4-dimethylcyclopentane-1-carboxylate **23** in CDCl$_3$.

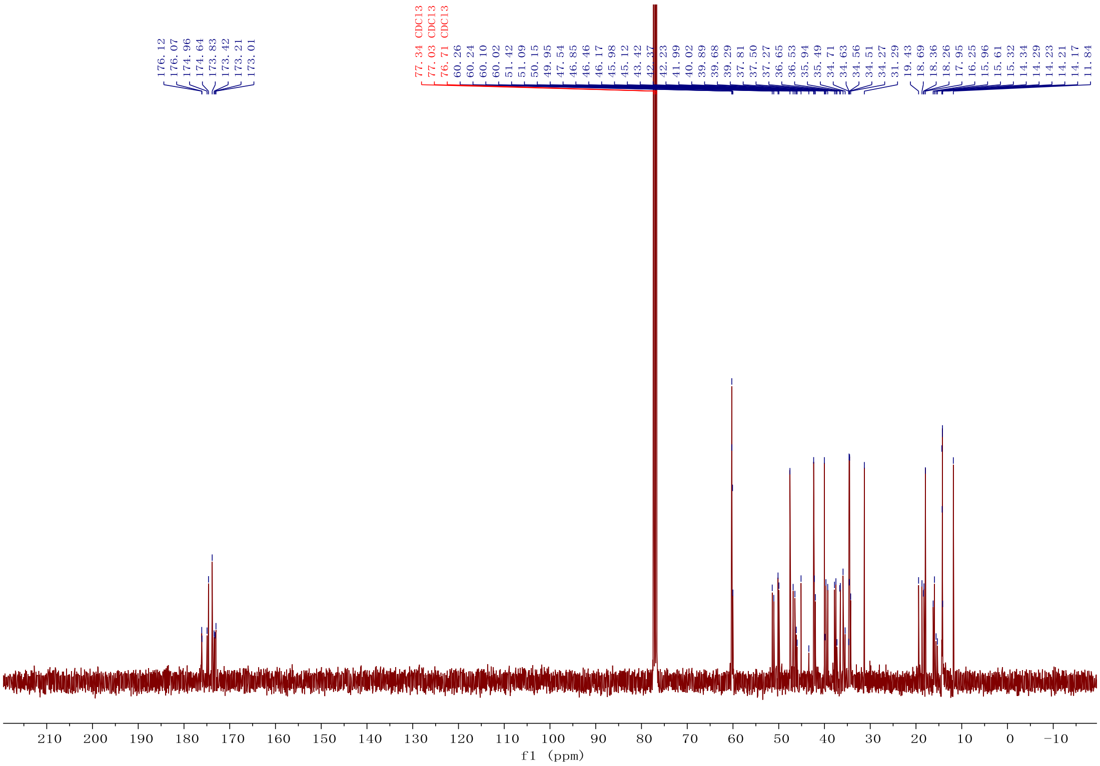

Figure S14. EI-MS spectrum of ethyl 3-(carbethoxymethyl)-2,4-dimethylcyclopenta-1,3-diene-1-carboxylate **22**.

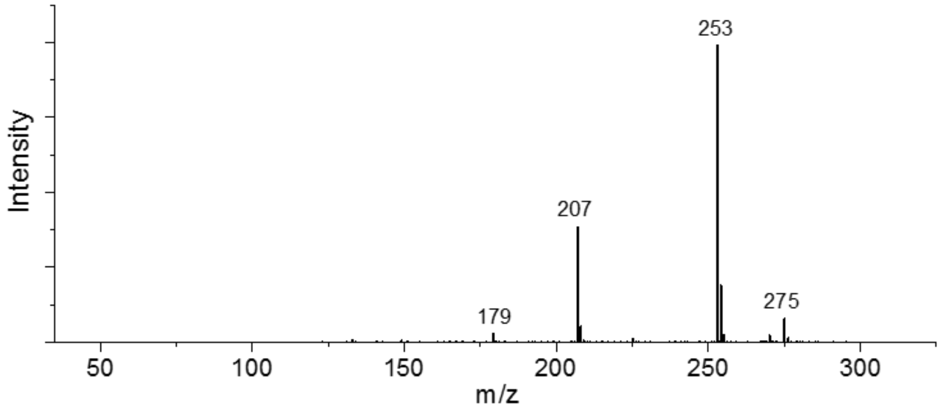

Figure S15. EI-MS spectrum of ethyl 3-(carbethoxymethyl)-2,4-dimethylcyclopentane-1-carboxylate **23**.

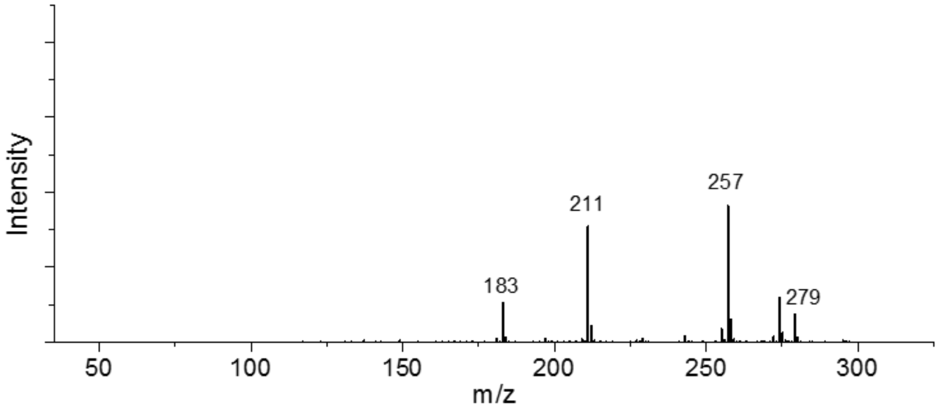

References used in ESI

[S1] M. Pyda, E. Nowak-Pyda, J. Heeg, H. Huth, A. A. Minakov, M. L. Di Lorenzo, C. Schick, B. Wunderlich, *J. Polym. Sci., Part B: Polym. Phys.*, **2006**, *44*, 1364-1377.

[S2] W. J. Jackson, J. J. Watkins (Eastman Kodak Company), US 4,600,768, **1986**.

[S3] T. H. Ng, H. L. Williams, *Makromol. Chem.*, **1981**, *182*, 3323–3330.

[S4] J. Thiem, H. Lueders, *Polym. Bull*., **1984**, *11*, 365-369.

[S5] R. Storbeck, M. Ballauff, *J. Appl. Polym. Sci.*, **1996**, *59*, 1199-1202.

[S6] Y. Jiang, A. J. J. Woortman, G. O.R. Alberda van Ekenstein, K. Loos, *Polym. Chem.*, **2015**, *6*, 5198-5211.

[S7] S. Thiyagarajan, W. Vogelzang, R. J. I. Knoop, A. E. Frissen, J. van Haveren, D. S. van Es, *Green Chem.*, **2014**, *16*, 1957-1966.

[S8] R. Storbeck, M. Ballauff, *Polymer*, **1993**, *34*, 5003-5006.

[S9] T. Debuissy, E. Pollet, L. Avérous, *Polymer*, **2016**, *99*, 204-213.

[S10] J. J. O'Malley, W. J. Stauffer, *J. Polym. Sci. Polym. Chem. Ed.*, **1974**, *12*, 865–874.